Sustainable Energy, Grids and Networks 38 (2024) 101359

Contents lists available at ScienceDirect

Sustainable Energy, Grids and Networks

journal homepage: www.elsevier.com/locate/segan

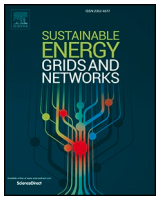

Quantifying power system frequency quality and extracting typical patterns within short time scales below one hour

Younes Mohammadi [a,*], Boštjan Polajžer [b], Roberto Chouhy Leborgne [c], Davood Khodadad [a]

[a] Department of Applied Physics and Electronics, Umeå Universitet, Umeå 90187, Sweden
[b] Faculty of Electrical Engineering and Computer Science, University of Maribor, Maribor 2000, Slovenia
[c] Universidade Federal do Rio Grande do Sul, Osvaldo Aranha, 99, Porto Alegre RS-90035-190, Brazil

ARTICLE INFO

Keywords:
Quantifying power system frequency quality
Statistical indices
Pattern extracting
Machine learning
Short time scales
Renewable energy sources

ABSTRACT

This paper addresses the lack of consideration of short time scales, below one hour, such as sub-15-min and sub-1-hr, in grid codes for frequency quality analysis. These time scales are becoming increasingly important due to the flexible market-based operation of power systems as well as the rising penetration of renewable energy sources and battery energy storage systems. For this, firstly, a set of frequency-quality indices is considered, complementing established statistical indices commonly used in power-quality standards. These indices provide valuable insights for quantifying variations, events, fluctuations, and outliers specific to the discussed time scales. Among all the implemented indices, the proposed indices are based on over/under frequency events (6 indices), fast frequency rise/drop events (6 indices), and summation of positive and negative peaks (1 index), of which the 5 with the lowest thresholds are identified as the most dominant. Secondly, k-means and k-medoids clustering methods in a learning scheme are employed to identify typical patterns within the discussed time windows, in which the number of clusters is determined based on prior knowledge linked to reality. In order to clarify the frequency variations and patterns, three frequency case studies are analyzed: case 1 (sub-15-min scale, 10-s values, 6 months), case 2 (sub-1-hr scale, 10-s values, 6 months), and case 3 (sub-1-hr, 3-min values, the year 2021). Results obtained from the indices and learning methods demonstrate a full picture of the information within the windows. The maximum value of the highest frequency value minus the lowest one over the windows is about 0.35 Hz for cases 1 and 2 and 0.25 Hz for case 3. Over-frequency values (with a typical 0.1% threshold) slightly dominates under-frequency values in cases 1 and 2, while the opposite is observed in case 3. Medium fluctuations occur in 35% of windows for cases 1 and 2 and 41% for case 3. Outlier values are detected using the quartile method in 70% of windows for case 2, surpassing the other two cases. About six or seven typical patterns are also extracted using the presented learning scheme, revealing the frequency trends within the short time windows. The proposed approaches offer a simpler alternative than tracking frequency single values and also capture more comprehensive information than existing approaches that analyze the aggregated frequency values at the end of the specific time windows without considering the frequency trends. In this way, the network operators have the possibility to monitor the frequency quality and trends within short time scales using the most dominant indices and typical patterns.

1. Introduction

1.1. Problem description and literature review

Frequency is a measure of power system balance; hence, it should be controlled. Different control levels are applied in different time frames, traditionally divided into 10–30 s for the primary, 10–20 min for the secondary, and 20 min-1 h for the tertiary control level [1]. The response time of converter-interfaced control units is much faster, i.e., in a time frame of 2 s or less [2]. Frequency is supposed to be within a target range around a nominal value, typically 50 Hz or 60 Hz, which is crucial for the power system's reliability. In cases of large and fast frequency variations, not only frequency variation should be limited, but also the Rate of Change of Frequency (RoCoF) to prevent equipment failure, cascaded tripping of power plants, and possibly loss of service [3–5]. As a standard method, the power system frequency measurement refers to the

* Corresponding author.
E-mail address: Younes.mohammadi@umu.se (Y. Mohammadi).

https://doi.org/10.1016/j.segan.2024.101359
Received 9 June 2023; Received in revised form 13 March 2024; Accepted 21 March 2024
Available online 26 March 2024

reiteration rate of the voltage signal in a particular location, where a zero-crossing method is commonly used, as explained in IEC 61000–4–30 [6]. Within interconnected systems such as the Nordic synchronous area (including Norway, Finland, Sweden, and the eastern part of Denmark), the frequency measurement values at multiple locations are very similar in normal conditions (less than a few mHz apart) with possible time shifts due to clock differences on the measuring devices. However, the time lag is also resolved using the phase measurement units (PMUs) [7,8], which are capable of reporting frequency and RoCoF synchronously with a high resolution of 20 ms in 50 Hz systems. According to the frequency evaluation in the Nordic area, using the data collected with PMUs [9], the maximum absolute RoCoF exceeds 0.1 Hz/s for 20% of recorded disturbances.

The quality of "power system frequency" or "voltage frequency" can be explained by two definitions: (a) variation of frequency from its rated value and (b) the power grid's capability to maintain a balance between generation and consumption. Frequency quality can be quantified based on both definitions by considering frequency quality indices for a predefined period [10]. Frequency variations are typically not a concern for the end-user customers and their grid-connected equipment; however, the frequency deviations are addressed as part of the "power--quality" standards IEC 61000–4–30 [6] and EN 50160 [11]. According to [11], the 10-s time resolutions should be used for frequency measurements, and the average frequency value for interconnected systems must be within the range of 49.5–50.5 Hz for 99.5% of the time (a year). Furthermore, the Nordic grid code [12] and the European Commission Regulation for the Nordic synchronous area [1] require that frequency must be within the standard range of 49.9 and 50.1 Hz during normal conditions. Considering different thresholds for higher and lower frequency values, over- and under-frequency events can occur in a given period of time, such as one year [13]. In 2021, 221 incident classification scale (ICS) events with scales 0–3 were reported in the Nordic synchronous area, of which 214 were events with a scale 0, and seven events were with a scale 1 [14]. The North American reliability council (NERC) also keeps statistics on the 60 Hz frequency quality in the four interconnected systems in North America [15]. Steady-state frequency variations can be quantified by indices such as the average or standard deviation over one year. A threshold can also be considered to detect the number of times the steady-state frequency exceeds it. In the power-quality field, the steady-state disturbances (such as harmonics/inter-harmonics [16–19]) and sudden events (such as voltage dips [20–23]) are distinguished and different indices are defined. Similarly, the frequency events due to the sudden imbalance between generation and consumption can be distinguished from steady-state frequency disturbances (variations) [24]. However, a minimum threshold must be assigned to conclude a frequency quality index.

The frequency quality indices are typically only considered over a specific period (time window), such as one year or monthly. For instance, [8] reports the frequency quality indices and disturbances in the Nordic system during 2021 using a time resolution of 0.1 seconds or aggregated over 1 second. Furthermore, electricity power markets typically use 15-min intervals for recording frequency measurements, but they are beginning to switch to 1-hour intervals [25–27]. Grid codes [1,15] also use frequency values with time resolutions of 1, 10, or 15-min, where aggregated, i.e., averaged frequency values, are used to determine frequency quality and control performance indices over a large time scale (time window) of 1-year or 1-month. However, there is a lack of literature quantifying frequency quality regarding variations, fluctuations, and events for specific time windows such as sub-5-min, sub-15-min, sub-30-min, and/or sub-1-hr. Many variations, events, fluctuations, out-of-range values, and detectable trends occur below the 15-min or 1-hr time scales for several reasons, such as the unbalance between generation and demand, which may result from load disconnecting, generator and/or line tripping. A review of the detection of frequency events in power systems is done in [28], highlighting the importance of small-time scales. Moreover, power system operation is becoming increasingly flexible due to market-based activities and the fast operation of converted-interfaced units. Therefore, aggregated frequency values at fixed times of 15-min or 1-hr may filter out important information on frequency quality and trends over a monthly or yearly time scale. Consequently, there is a lack of knowledge and information regarding the short-time scales and a need to shorten the time scales from monthly/yearly, including the time resolutions with aggregated values over 15-min or 1-hr, to short time scales as sub-15-min or sub-1-hr with higher real-time resolutions in second or few minutes. Therefore, there is a need to introduce indices that can quantify variations, events, fluctuations, and typical patterns that may exist in 15-min or 1-hr time windows. Article 131, "Frequency quality evaluation criteria" in [1], shows that the current indices are as: the mean value, the standard deviation, single percentiles as 1, 5, 10, 90, 95, and 99th and few more. Hence, introducing more proper indices within short time scales is important to give a better picture of frequency changes and trends. Moreover, researchers in this field should also investigate how the operation of different types of control units, balancing processes and electricity markets is reflected through the frequency indices and typical patterns within the considered short time scales.

Quantifying fast variations in root mean square (rms) [29] and harmonic [30] voltages have been studied in sub-10-min time scales. The importance of this time scale has been discussed, and some statistical indices were proposed. However, there is no literature regarding quantifying frequency variations for time scales such as sub-15-min or sub-1-hr. Since recording the frequency measurements for high resolutions such as 20 ms, 1 s, or 10 s, even for specific windows, generates a huge amount of data, "big data" [31–34], introducing frequency-quality statistical indices can also avoid the need to save all high-resolution frequency values. Instead of saving all high-resolution frequency values, the proposed indices can be calculated and saved using the online high-resolution values within the windows.

Time series clustering, or so-called "pattern extraction", is investigated in several kinds of literature. Examples include big data clustering [32], shape-based clustering [35], clustering using Distance Time Wrapping [36], k-means and k-medoids clustering methods [37], and an improved version of k-means in [38]. However, the application of the clustering methods is limited, especially for power-quality data. The studies in the literature include a time series clustering to extract knowledge existing in energy consumption data [39], X-means clustering, rival penalized expectation maximization used as part of detection and clustering of unknown classes of voltage transients [40], and detecting voltage dips and spikes using clustering large applications' algorithms [41]. A review of artificial intelligence applications regarding different aspects of harmonic analysis, including data clustering, has been reported in [42]. In addition, detecting abnormalities and events and clustering of harmonic data and events have been comprehensively studied in [43]. Very few studies have paid attention to the short-time scales. The typical "sub-10-min" patterns of rms voltages were extracted using an unsupervised learning method, which used kernel principal component analysis (KPCA), tracked by a k-mean clustering applied to the data regarding a location in northern Sweden [44] and multiple location data worldwide [45]. The study in [46] identified potential patterns of the occurrence of power system disturbances over two years. Previous works, such as [47,48], have focused on unsupervised learning methods for classifying electrical customer load patterns. Recently, a study [49] reviewed the power system frequency analysis (not patterns) using deep learning methods. However, there have been no reports on identifying patterns in frequency measurements for both long-time and short-time scales, such as sub-15-min or sub-1-hr. Extraction of frequency patterns using unsupervised machine learning methods, such as [44,45,50], can also seek the trend of frequency variations within the windows. However, finding the number of clusters (groups) over data is an issue that requires some pre-knowledge on the frequency values within the windows.

1.2. Contribution, input cases, and organization of the paper

Given the research and practical gaps highlighted in the previous section, the main contributions of this paper are listed as follows:

- Laying a solid foundation for a new standardization in defining frequency quality and extracting frequency patterns, focusing on short time scales and including higher time resolutions of frequency values.
- Quantifying frequency quality in terms of variations, fluctuations, events, and outliers that can occur in frequency values within short time scales, exceeding the existing indices in the grid codes.
- Utilizing 23 established statistical indices and proposing 13 frequency quality indices applicable for short time scales (a total of 36 indices).
- Showing the independence of the statistical indices concerning the lengths of short time scale windows (5 min, 10 min, 15 min, 1 hour, etc.) and time resolutions.
- Proposing the most dominant frequency quality indices out of the 36 considered indices.
- Implementing an unsupervised learning scheme using k-means and k-medoids clustering methods to short time scale windows to extract existing typical patterns. The number of clusters is determined based on prior knowledge related to the physical reality of frequency values within the windows, as well as the reasonable separation of clusters visualized in a 2D space.
- Compressing and converting frequency windows using the statistical indices and extracted patterns to avoid storing each individual high-resolution frequency sample in a big data space.

To better clarify the frequency variations and trends, three input case studies are analyzed in this paper; the first and second use 10-s recorded measurements for the short time scale such as sub-15-min and sub-1-hr windows, respectively, while the third case study uses 3-min resolution data available on the Finnish grid company website (Fingrid) for sub-1-hr windows. Besides quantifying the frequency quality and extracting typical patterns using the statistical indices and clustering methods, 10 of the 23 existing indices and 5 of the 13 proposed indices have been selected as the most dominant ones (a total of 15 out of 36). Six typical patterns (for input cases 1 and 2) and seven (for case 3) are also extracted to show the trend of frequency values within the windows.

The rest of the paper is organized as follows: 2 presents the approach of the study in terms of quantifying variations, fluctuations, events, and outliers using statistical indices proposed by us or selected from existing literature and extraction of frequency patterns using an unsupervised learning schema, all within short time scales. 3 introduces the employed datasets and three extracted input cases under our studies with sub-15-min (10-s time resolution) and sub-1-hr (10-s and 3-min resolution) windows. This section also shows some examples of frequency variations among the input cases. In 4 the results are shown for both statistical indices and pattern extraction. A comprehensive discussion of the statistical indices and learning results as well as recommendations for future studies, are made in 5, and finally, 6 concludes the paper.

2. The approach of the study

When considering frequency records within short time windows, it becomes necessary to define certain indices to quantify frequency quality and develop an approach to extract the possible typical pattern of variations. The following sections, 2.1 and 2.2, outline the methodologies employed to achieve these objectives. It is important to note that the statistical indices discussed/proposed in the subsequent sections are independent of specific short window lengths and time resolutions because of their statistical nature. However, this is distinct from the process of selecting threshold values, which entails careful consideration and often involves a thorough examination of the values within the specific window lengths over an extended period. The same holds for selecting the number of clusters in a data-driven manner, which could be dependent on the frequency data within specific window lengths over a certain period, such as weekly, monthly, every six months, or yearly. However, the framework for extracting the typical patterns is the same for any window length or time resolution of frequency instants. In our study, we have selected sub-15-min and sub-1-hr windows as well as 10-s and 3-min frequency samples (which will be explained in 5.3). However, some of the indices from [29], which utilized a 10-min window length and 1-s resolution, can be readily applied in our study for different window lengths and time resolutions.

2.1. Quantifying the frequency quality within the short time windows

2.1.1. Indices to quantify the variations as a range in values

The indices considered and suggested for this category include the following:

- Mean, maximum, and minimum of the values for frequency (f) and the RoCoF[1] $= \mathrm{df/dt}$ within the windows.
- Difference between two percentiles within the windows ("R100, R98, R90, R80". The references [29] and ([45], Table A1) explain the indices that were applied on "sub-10-min" rms voltage variations).
- "Over-deviations" from the frequency rms value within the windows ("P100, P99, P95, P90" [29] and ([45], Table A1).
- "Under-deviations" from the frequency rms value within the windows ("P0, P1, P5, P10" [29] and ([45], Table A1).
- Standard deviations (Std) as non-sliding-window rms on frequency samples' "very short variations". This index shows the deviation of frequency samples from the mean value of the current window.

2.1.2. Indices to quantify the events

The indices suggested for this category require some triggering mechanisms. Note that the events here consider steady-state variations and the sudden drops/rises exceeding a high/low threshold. The indices are as follows:

- The number of over-frequencies (OF) exceeding a high threshold as nominal frequency plus 0.1%, 0.2%, and 0.3% of nominal frequency within the windows, i.e., the values more than $50\,Hz + 0.1\%/0.2\%/0.3\%$ (NOF1, NOF2, NOF3).
- The number of under-frequencies (UF) exceeding a low threshold as nominal frequency minus 0.1%, 0.2%, and 0.3% of nominal frequency within the windows, i.e., the values less than $50\,Hz$ - 0.1%/0.2%/0.3% (NUF1, NUF2, NUF3).
- The number of fast frequency rises (FFR) exceeding a high threshold for RoCoF. The thresholds can be selected based on existing time resolutions as well as the RoCoF values. Sudden frequency events as rises are quantified by this index.
- The number of fast frequency drops (FFD) exceeding a low threshold for the RoCoF, with the same thresholds assigned for the FFR in negative sign (NFFD1, NFFD2, NFFD3). Sudden frequency events as drops are quantified by this index.
- Short timescale very short variations (VSV [51]), specific to the short time windows, as sliding-window rms on frequency samples' very short variations.

The thresholds for NOF/NUF have been selected based on the operation limits regarding the over- and under-frequency events defined in NERC [15]. The thresholds for NFFR/NFFD need to be chosen

[1] RoCoF is better to be calculated from high-resolution frequency samples, however, the goal in this study is to show how the RoCoF value with the existing time-resolutions can be employed as frequency-quality indices within specified window length.

according to the RoCoF values for each input case to cover a meaningful range of sudden events within the selected windows. Both sudden events (drop/rise) and steady-state variations (constant/upward/downward) with a trigger mechanism can be quantified by the NOF/NUF index. VSV can also be used as an index to quantify events since it shows that frequency samples deviate more than a certain from the mean over the last window corresponding to that frequency value. This index integrates all the specific windows defined for an input case.

2.1.3. Indices to quantify the fluctuations

The index suggested for this category is a summation of the following criteria:

1. The number of positive peaks of frequency values ($f(t)$) that exceed their immediate neighboring values (f (t-1), f (t+1)) within the windows by at least a high threshold.[2] These positive peaks are detectable as shown in Eq. (1):

$$[f(t) > f(t-1) \& f(t) > f(t+1) \& |f(t) - f(t-1)| > Thr \& |f(t) - f(t+1)| > Thr] \tag{1}$$

2. The number of negative peaks of frequency values ($f(t)$) that exceed their immediate neighboring values ($f(t$-1), $f(t$+1)) within the windows by at least a low threshold (equal to the high threshold). These negative peaks are detectable, as shown in Eq. (2):

$$[f(t) < f(t-1) \& f(t) < f(t+1) \& |f(t) - f(t-1)| > Thr \& |f(t) - f(t+1)| > Thr] \tag{2}$$

Three levels of fluctuations are assigned to each window according to the summation of a number of positive and negative peaks (SNPNP) as low, medium, and high fluctuation, as shown in Eq. (3). The coefficients a and b correspond to different percentages to show the fluctuation levels, and it is recommended to be chosen based on the time resolutions existing in the input cases.

$$\begin{cases} Low \quad fluct., & SNPNP < a \times window \quad len. \\ Medium \quad fluct., & a \times window \quad len. < SNPNP < b \times window \quad len. \\ High \quad fluct., & SNPNP > b \times window \quad len. \end{cases} \quad 0 < a, b < 1, a < b \tag{3}$$

2.1.4. Indices to quantify the outliers

Outliers are considered as the values that stand out in the overall pattern of the values within the windows, according to the statistics. Although some of the values, such as FFRs/FFDs, may not be considered outliers in reality, we are trying to show some out-of-range values within the windows apart from the other values to show the frequency variations. Three methods have been considered to quantify the number of outliers within the windows [52].

- *Median method*: The number of values out of the median of window ± 3 × scaled medium absolute deviation (MAD) (Noutlier1).

$$Scaled \quad MAD = -1 \Big/ \sqrt{2} Cmedian \quad (|f_i - median(f_i)|) \tag{4}$$

In which *efi* is the inverse complementary error function and by the function *erfcinv* in MATLAB, $C = efi(3/2) = -0.4769$.

- *Mean method*: The number of values out of mean of window ± 3 × Std of a window (Noutlier2).
- *Quartiles method*: The number of values out of $[Q1 - 1.5IQR \; Q3 + 1.5IQR]$ (Noutlier3).

In which Q1 and Q3 are 25th and 75th percentiles, and IQR is Q3-Q1.

2.2. Extracting the frequency patterns within the short time windows

In order to extract the frequency variation patterns within the short time windows, a framework is presented as shown in Fig. 1. To make an equal contribution to each n feature in the input matrix X, a Z-score normalization is applied as $[(x_i - \mu(x_i))/\sigma(x_i)]$ to each x element of matrix X over whole m samples, whereas μ, and σ are the mean and standard deviation of each row of X. Since each row of matrix X is as a time series, row normalization [53] has been used in which the more real patterns were extracted finally. Normalization can improve the generalization of the learning in comparison with no-normalized data. To cluster frequency datasets shaped in a matrix X, two well-known clustering methods, k-means, and k-medoids [54–56], are used to label each row of matrix X as 1, 2, …, K.

The implementation steps of the two methods are as follows:

The *k-means*++ and *k-medoids*++ initialization techniques [57] find out K initial cluster centers, i.e., centroids in k-means (Ctd_j)/medoids in k-medoids (Mdd_j), in an effective way.

Each input sample $x_i (i = 1, \ldots, m)$ is assigned to a cluster (ω_{ij}) with the shortest 'distance' (d_{ij}) to one of the ($j = 1, \ldots, K$)centroids/medoids with n dimension, Eq. (5).

$$\omega_{ij} = \begin{cases} 1, & if \quad j = arg\min_j d_{ij} \\ 0, & otherwise \end{cases} \tag{5}$$

The k-means/k-medoids minimize Eq. (6) the summation of the distances of each x_i to its Ctd_j/Mdd_j.

$$\min \sum_{j=1}^{K} \sum_{i=1}^{m} \omega_{ij} d_{ij} \tag{6}$$

Centroids in k-means (Ctd_j) as a mean of all samples (which may not be a real sample) within a cluster are then updated once all vectors x_i are assigned, Eq. (7).

$$Ctd_j = \frac{\sum_{i=1}^{m} \omega_{ij} x_i}{\sum_{i=1}^{m} \omega_{ij}}, j = 1, 2, \ldots, K \tag{7}$$

Medoids in k-medoids ($Mdd_j \in x_i$) are a representative sample within a cluster rather than the mean in k-means. For each

[2] This tthreshold refers height difference between a peak and its neighbors. Althought the frequency control has a certain dead-band, it is however needs to be selected based on the available time resolutions in the input cases in order to show the fluctuations clearer.

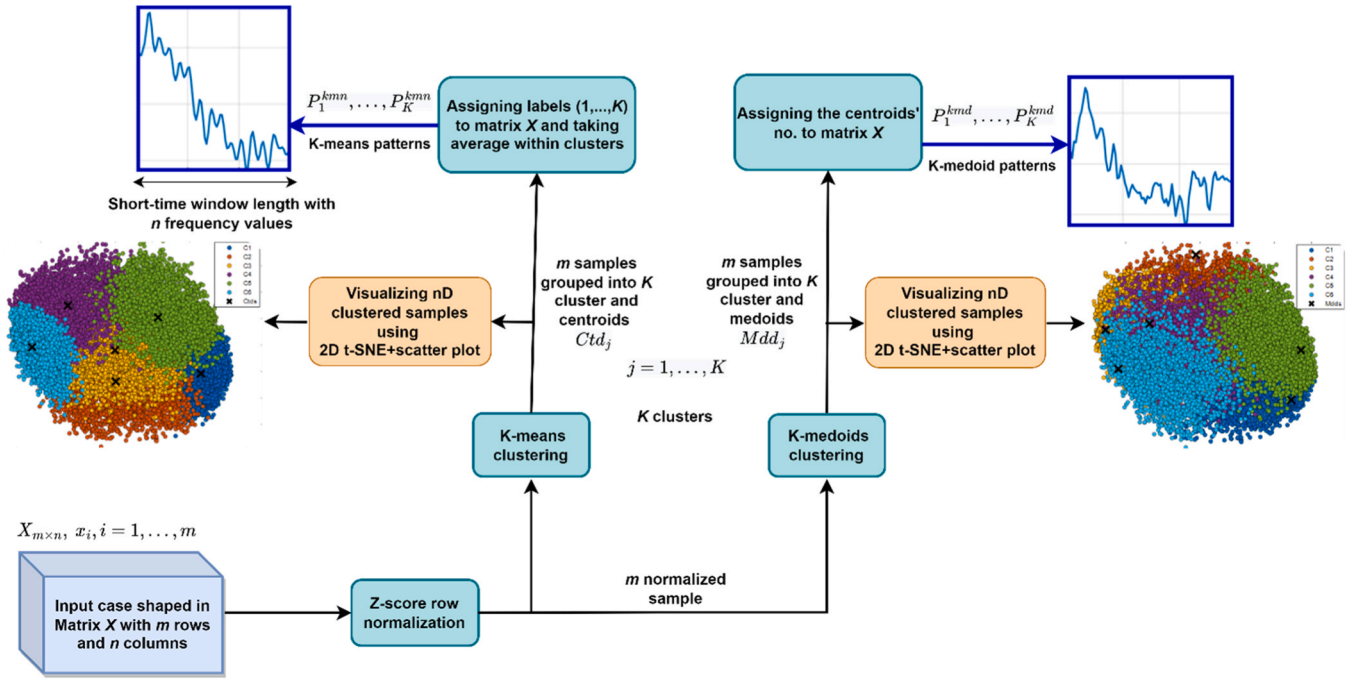

Fig. 1. Process of the clustering techniques for extracting typical patterns of frequency variations within short time windows.

representative Mdd_j and each x_i which is not a medoid, the Mdd_j and x_i are swapped. Then, steps 2 and 3 are repeated. If Eq. (6) is more than that in the previous iteration, the swap is then ignored.

Steps 2, 3, and 4.1 for k-means and 2, 3, and 4.2 for k-medoids are repeated until convergence (i.e., no new cluster centers or reaching maximum iteration).

The distance used d_{ij} in the k-means/k-medoids is the squared Euclidean $\|x_i - Ctd_j\|_2^2$ / $\|x_i - Mdd_j\|_2^2$. A t-Distributed Stochastic Neighbor Embedding (t-SNE) function [58] plus a scatter plot is applied for visualizing the clustered n-dimensional samples (x_i^{nD}) and Ctd_j/Mdd_j into two dimensions.

In the next step, to extract the patterns, the obtained labels for the samples on the output of the clustering blocks (from 1 to K), along with the medoid's sample numbers, are picked up and assigned to the samples in the input space. Then, centroids are obtained by averaging input samples within clusters (P_1^{kmn}, …, P_K^{kmn}), and medoids are defined in input space by using the existing medoid's sample numbers (P_1^{kmd}, …, P_K^{kmd}). The number of selected clusters (will be explained in 4.2) are 6, 6, and 7 for cases 1, 2, and 3, respectively, as written in Fig. 1.

3. Employed frequency datasets, prepared input cases, and examples of variations

3.1. Employed frequency datasets

This study uses two different frequency measurement datasets as time series of 10 s and 3 min values. The first dataset (10-s values) is extracted from the six-month measurements recorded in an apartment in northern Sweden for December 2021, January-March 2022, and June-July 2022. A Metrum PQsmart portable monitor (the same one used in our previous works [44,45]) connected to a wall outlet at 220 V and 50 Hz was used for the measurements in which the best frequency resolution is 10 s. 10 s also comes from European voltage characteristics and is also somewhat arbitrary. In fact, the frequency events due to the loss of a large production unit will take place at a shorter time scale. All measurements follow IEC 61000–4–30 Class A[3] and the requirements defined in [1]. The second dataset (3 min values) is obtained from the measurements reported on the Finnish grid company website [59] for the entire year 2021; however, one may use diverse time resolutions. The first and second datasets are plotted in Fig. 2, and it is clear that the 10-s measurements (Fig. 1a and b) can be used to quantify the frequency variations. A frequency value of 48.97 Hz was also recorded on 08–05–2022, 06:33:10 am, as marked by a red circle in Fig. 2a. Moreover, about 42% of frequency 10-s values (Fig. 2b) and 70% of 3 min values (Fig. 2d) are below 50 Hz.

Sections 3.2 and 3.3 give prepared input cases and random examples of variations happening within short-time windows, all obtained from the employed datasets explained in 3.1. From this point forward in this paper, the term 'short time scales/windows' will refer to time windows of sub-15-min and sub-1-hr. More explanation regarding the selection of window lengths, time resolutions, and preparation of these three input cases are assessable in 5.3.

3.2. Arranged input cases

A pre-processing was done on the datasets, and missing values were replaced with the average values of their previous and further values. Dividing the first dataset into 15-min and 1-hr windows, as well as the second dataset into 1 hr windows, generate a matrix $X_{m\times n} = [x_1, x_2, \ldots, x_m]^T$ with m rows showing the number of samples (windows) as $x_i = [x_{i1}, x_{i2}, \ldots, x_{in}], i = 1, \ldots, m$, including n features (dimensions) for three different input cases as follows:

- Input case 1, Time resolution =10 s, Window length=15 min, m=17568, n=90.
- Input case 2, Time resolution =10 s, Window length=1 hr, m=4392, n=360.

[3] A low pass filter as well as a "flagging" concept is used in this device so that the frequency measurements are in an acceptable range of 1 mHz.

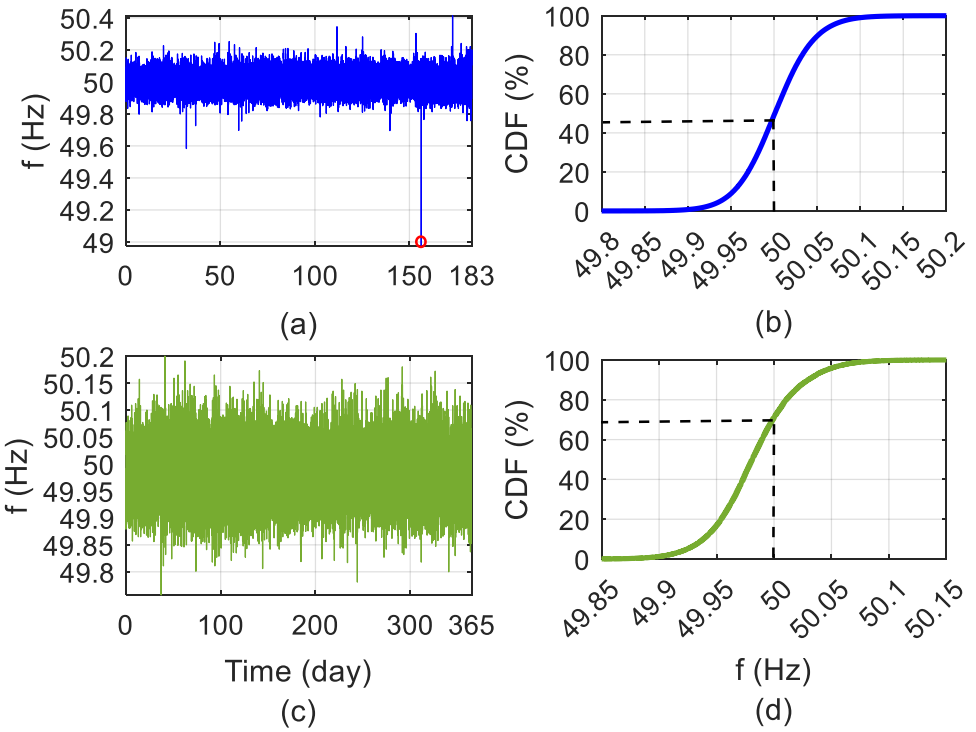

Fig. 2. Frequency measurements in terms of (a, b) 1-s time series and cumulative distribution functions (CDF) for the first dataset; (c, d) 3 min time series and CDF for the second dataset.

- Input case 3, Time resolution =3 min, Window length=1 hr, m=8760,[4] n=20.

Input cases 1 and 2 are candidates to discover the variations, events, fluctuations, outliers and typical patterns that can happen for higher-resolution frequency values in sub-15-min and sub-1-hr intervals of selected months. Input case 3 is also a representative to demonstrate which kind of variations and/or patterns are expected for the frequency values in sub-1-hr intervals for the entire year 2021.

3.3. Examples of variations in sub-15-min and sub-1-hr windows

Three random samples of variations in frequency values within the sub-15-min and sub-1-hr windows are shown in Fig. 3.

The examples correspond to the input cases 1 (1 s values in Figs. a, d, and g), 2 (1 s values in Figs. b, e and h), and 3 (3 min values in Figs. c, f, and i). By looking at all frequency recordings within the windows regarding the three input cases, which three random examples among all the windows are shown in Fig. 3, there are some visible observations such as sudden drops or rises in frequency values (more seen in 10 s values than 3 min values), slow drift of frequency towards a high value or a low value, fluctuations in frequency values, exceeding the frequency values from some possible thresholds, some outlier values (values that stand out from the overall pattern of the values in the windows) and some existing patterns (Table 6) of frequency values within the sub-15-min and sub-1-hr windows. Hence, the next section presents (a) frequency-quality indices to quantify the frequency variations, events, fluctuations, and outliers and (b) pattern extraction analysis by clustering methods to quantify the possible frequency patterns in sub-15-min and sub-1-hr windows. In general, all these observations show that first, the variations within the windows should not be neglected in terms of variations, events, fluctuations, and typical patterns. Second, some physical and electrical events, such as connecting/disconnecting the loads, may occur within these time windows.

[4] For the pattern extraction (4.2.3), some of the windows with constant values are removed from this dataset, hence, a dataset with m = 8680 windows are used there.

4. Results

4.1. Results of statistical frequency-quality indices

The results of statistical frequency-quality indices introduced in 2 are given in this section for the three input cases to bring more knowledge regarding the frequency variations, events, and fluctuations happening in sub-15-min (10-s resolutions) and sub-1-hr windows (10 s and 3 min resolutions). According to the Nordic grid code [12], in which the Swedish and Norwegian TSOs have the task of maintaining the frequency and time deviation within set limits, the allowable variations in the frequency values during the "normal conditions" is between 49.9 and 50.1 Hz, i.e., the frequency values deviate as 0 to ±0.1 Hz (maximum 0.2 Hz variation's range within a specified window) from the nominal frequency. This is also mentioned in the European Commission report for the Nordic area [1]. The box plots for the windows defined in the input cases 1, 2, and 3 in Fig. 4 show that the maximum/minimum frequency values in the input cases exceed the allowable standard ranges. Fig. 5 shows the mean, maximum, and minimum of the RoCoF values for the input cases. The results for input cases 1 and 2 are similar (a maximum of +34.9 mHz/s and −28.4 mHz/s is observed), and input case 3 shows different results (a maximum of about +54.33 mHz/min and minimum of −64 mHz/min). The results obtained from Fig. 5 will be used for the thresholds needed in the FFD and FFR indices introduced in 2.1.2.

The average values for the windows as well as the highest RoCoF for the samples shown in Fig. 3 are given in Table 1. Table 2 provides the thresholds used in this study for the indices introduced in 2.1. In the following, the results of the indices over all windows in the input cases 1, 2, and 3 are given in the form of histograms, probability density

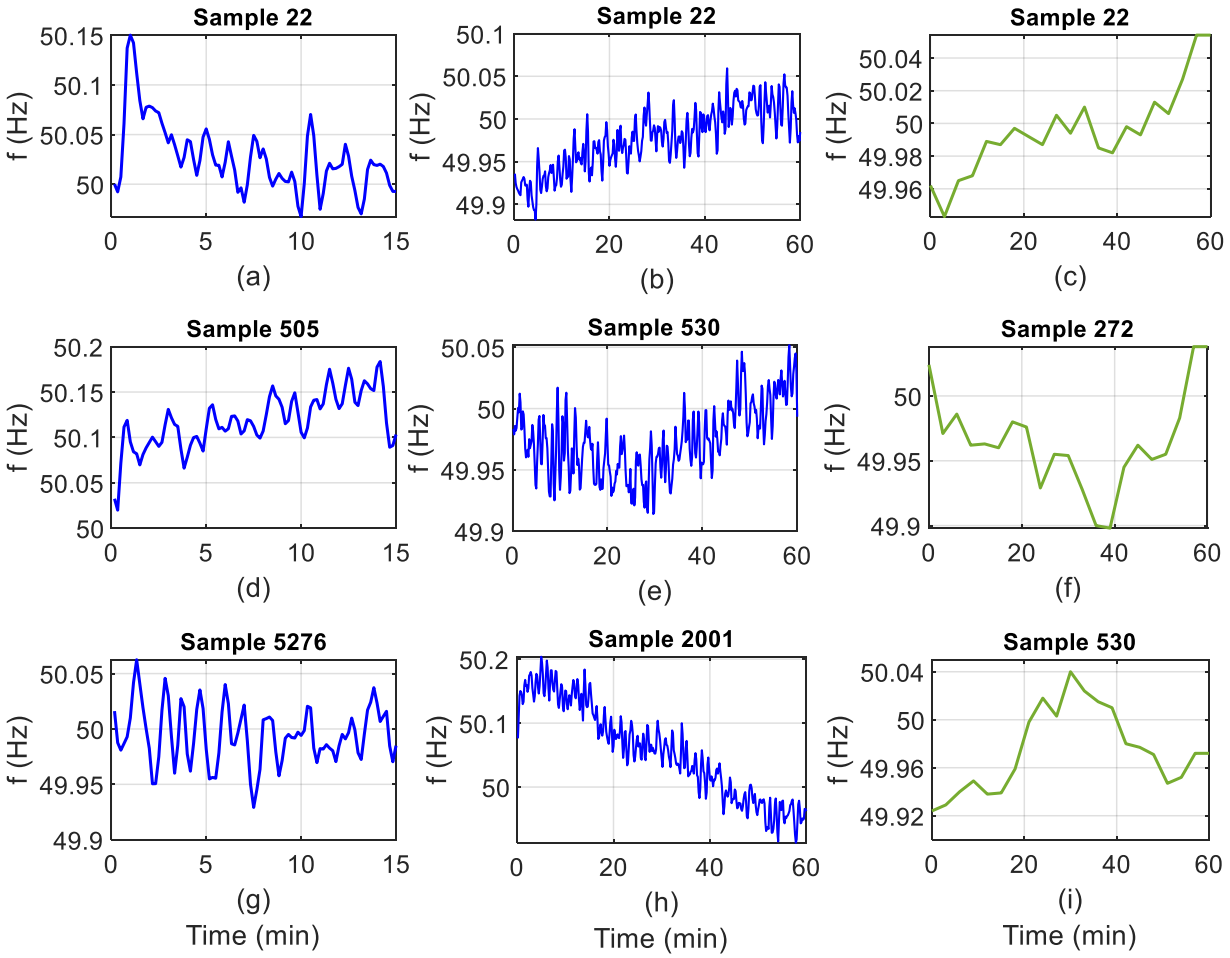

Fig. 3. Three random samples of frequency variations. (a, d, g) Input case 1; (b, e, h) Input case 2; (c, f, i) Input case 3.

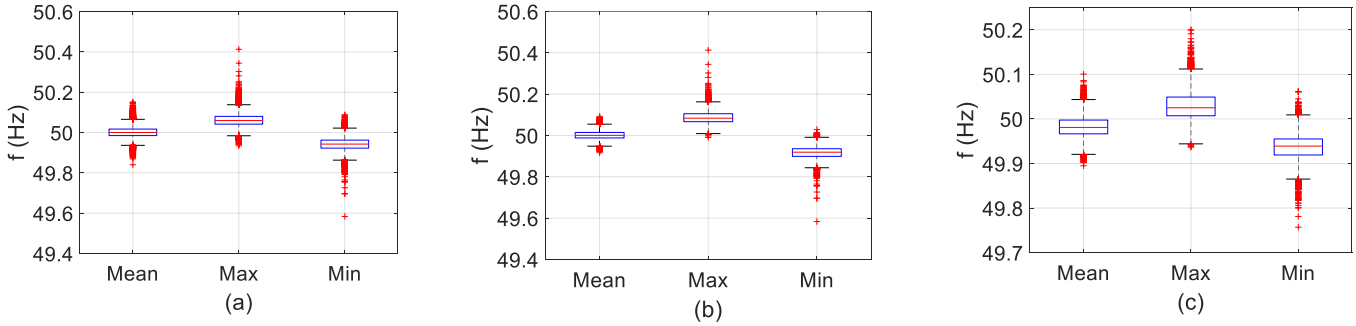

Fig. 4. Box plot of Mean, Max, and Min indices on the frequency values within the windows for (a) Input case 1; (b) Input case 2; (c) Input case 3. The event of 08–05-2022 in Fig. 2a is excluded.

functions (PDFs), and cumulative distribution functions (CDFs) curves. To fit a distribution to the histogram[5] data regarding the indices quantifying variations as a range in values and VSV, in the input cases 1, 2, and 3, a non-parametric kernel PDF is used for the distribution of the indices; hence, the median and average of the indices is not the same, as seen in Figs. 6, 10, and 14.

4.1.1. Input case 1

First, the results for the sample indices R100, P100, P0, and VSV, regarding the examples shown in Fig. 3 are given in Table 1. Then, the histograms fitted by a kernel PDF for the indices quantifying variations as a range in values and VSV within the windows in input case 1 are shown in Fig. 6. Fig. 6a shows that the frequency deviates by 0.05 Hz to 0.25 Hz within the sub-15-min windows with 10-s resolution, in which a range 0.2 Hz is allowable for the normal conditions designed for the Nordic area [1,12]. Almost 12%,[6] 10%, 8%, and 9% of the windows have values around the median for R100 (0.12 Hz), R98 (0.11 Hz), R90 (0.08 Hz), and R80 (0.06 Hz). The results of R100/R98 are far from the R90/R80, which shows there are not too many differences between the

[5] The number of bins equal to the square root of the number of samples m in the input cases 1, 2 and 3.

[6] The numbers are obtained from dividing vertical axes values per m.

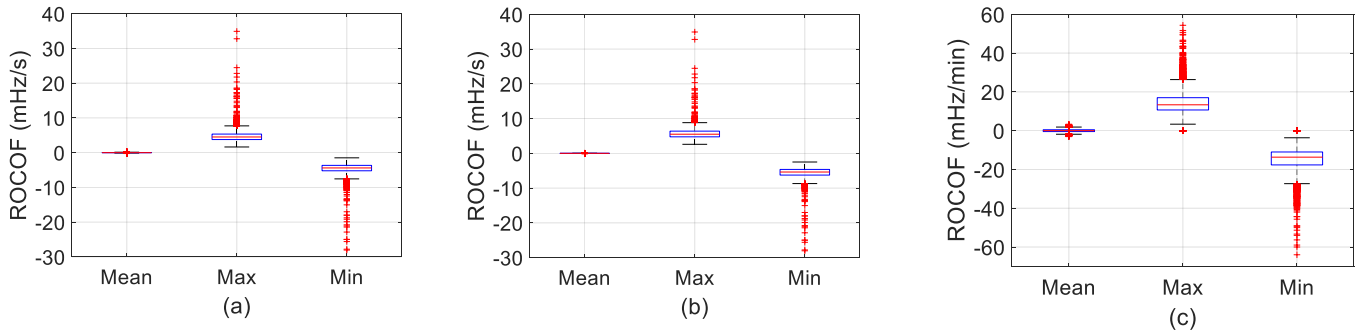

Fig. 5. Box plot of Mean, Max, and Min indices on the RoCoF values within the windows for (a) Input case 1; (b) Input case 2; (c) Input case 3. The event of 08–05-2022 marked in Fig. 2a is excluded.

Table 1
Some of the statistical frequency-quality indices for the samples shown in Fig. 3.

Indices	Input case 1			Input case 2			Input case 3		
	(a)	(d)	(g)	(b)	(e)	(h)	(c)	(f)	(i)
Mean (Hz)	50.03	50.12	49.99	49.98	49.97	50.06	49.99	49.96	49.97
Maximum RoCoF	7.7 (mHz/s)	5.17 (mHz/s)	4.5 (mHz/s)	5.25 (mHz/s)	4.36 (mHz/s)	4.63 (mHz/s)	9.00 (mHz/min)	18.33 (mHz/min)	13.00 (mHz/min)
R100 (Hz)	0.18	0.16	0.13	0.18	0.14	0.29	0.11	0.14	0.12
P100 (Hz)	0.12	0.07	0.07	0.08	0.08	0.15	0.06	0.08	0.07
P0 (Hz)	-0.06	-0.10	-0.07	-0.09	-0.06	-0.14	-0.05	-0.06	-0.05
VSV (Hz)	0.04	0.06	0.03	0.04	0.04	0.07	0.02	0.04	0.04
[NOF1, NOF2, NOF3]	[1,4,16]	[15,66,88]	[1,0,0]	[2,0,0]	[1,0,0]	[189,108,48]	[1,0,0]	[0,0,0]	[0,0,0]
[NUF1, NUF2, NUF3]	[0,0,0]	[0,0,0]	[2,0,0]	[83,6,0]	[74,0,0]	[22,0,0]	[1,0,0]	[5,2,0]	[7,0,0]
[NFFR1, NFFR2, NFFR3]	[1–3]	[2,1,0]	[4,0,0]	[3,1,0]	[2,0,0]	[4,0,0]	[0,0,0]	[2,2,0]	[2,0,0]
[NFFD1, NFFD2, NFFD3]	[1,0,0]	[2,0,0]	[4,0,0]	[3,0,0]	[3,0,0]	[4,0,0]	[0,0,0]	[2,2,0]	[2,0,0]
SNPNP	22	15	17	62	55	57	7	4	4
Level of fluctuations	Medium	Low	Low	Low	Low	Low	Low	Low	Low
[Noutlier1, Noutlier2, Noutlier3]	[3,4]	[1,2]	[0,0,0]	[0,0,0]	[0,0,0]	[0,0,0]	[1,0,2]	[1,0,4]	[0,0,0]

Table 2
The thresholds used for the indices introduced in 2.1.

Threshold	Values
High thresholds for (NFFR1, NFFR2, NFFR3)	+3.5, +5, and +6.5 (mHz/s) for cases 1 and 2; +10, +15, and +20 (mHz/min) for case 3
Low thresholds for (NFFD1, NFFD2, NFFD3)	+3.5, +5, and +6.5 (mHz/s) for cases 1 and 2; +10, +15, and +20 (mHz/min) for case 3
High threshold for SNPNP in Eq. (1)	0.01% of nominal frequency (5 mHz) for all cases
Low threshold for SNPNP in Eq. (2)	0.01% of nominal frequency (5 mHz) for all cases
Percentages a and b for SNPNP in Eq. (3)	$a = 20\%$, $b = 25\%$ for cases 1 and 2, $a = 40\%$ and $b = 60\%$ for case 3

highest and 99th percentiles, between the lowest and 1st percentiles, between 90th and 95th percentiles, and between 5th and 10th percentiles of the indices over the windows. However, there are differences between the highest and/or 99th percentile and lowest/1st percentile, or between 90th/95th and 5th/10th percentiles. These observations, along with the differences in the histograms, confirm the variations happening during the sub-15-min windows. Comparing the results of the over-deviation indices as P100, P99, P95, and P90 in Fig. 6b with the indices in Fig. 6a shows that a factor of two needs to be considered in a comparative analysis (see, for example, the differences in the median values). When comparing Fig. 6c (under-deviation indices) with Fig. 6b (over-deviation indices), the absolute values seem similar (see, for example, the median values). However, to have a two-by-two closer comparison for all the windows, Table 3 gives the number of windows in which the difference between over-deviation and under-deviation values deviates more than 0.01 Hz. As seen in this table, the over-deviations dominate a little more than under-deviations for input case 1. For about 50% of the samples, the difference for the indices P0-P100 or P1-P99 is within 0.01 Hz. Variations from the average over the current window (Std) or over the last windows (VSV) are shown in Fig. 6d, which shows that VSV values are higher. The maximum VSV (100th percentile) observed is about 0.08 Hz, while Std. gets around 0.06 Hz. Since VSV considers the variations happening during the previous window (for each frequency value within a window), it gives more information than Std. For example, a sudden rise or drop in frequency values will show a higher VSV value than the Std.

The number of over-frequency and under-frequency values for the samples shown in Fig. 3 are given in Table 1. A CDFs on all the windows in input case 1 are shown in Fig. 7a and demonstrate that OF/UF values with the threshold 0.1% are common, and almost 25% of the windows have experienced it at least 9 times (10% of the window length). 90% and 99% of the windows have no OF/UF due to the threshold 0.2% or 0.3%, which shows these two thresholds are less common. Fig. 7a also shows that the NOF1 and NUF1 for almost 60% of the windows have varied between 1 and 80 (89% of window length). The difference between NOF1 and NUF1 is higher for the high percentiles from 80th up to 95th, so for the 90th percentile, NUF1 is 7 units higher than NOF1. Accordingly, the number of windows with NUF higher than NOF is slightly higher. The number of fast-frequency rise and drop values for the samples shown in Fig. 3 is given in Table 1. The CDFs on all the windows are also shown in Fig. 7b, which shows that FFR/FFD values with the threshold of 3.5 mHz/s are common because almost 80% of the windows have experienced it up to 5 times. The values with the threshold of 5 mHz/s are relatively common since 30% of the windows have at least one, and the values with a threshold of 6.5 mHz/s are less common since almost 92% of the windows have no FFR and FFD. The CDFs for the number of FFD/FFR are very similar, which may mean for an FFD in a window, there must be an FFR too and in opposite.

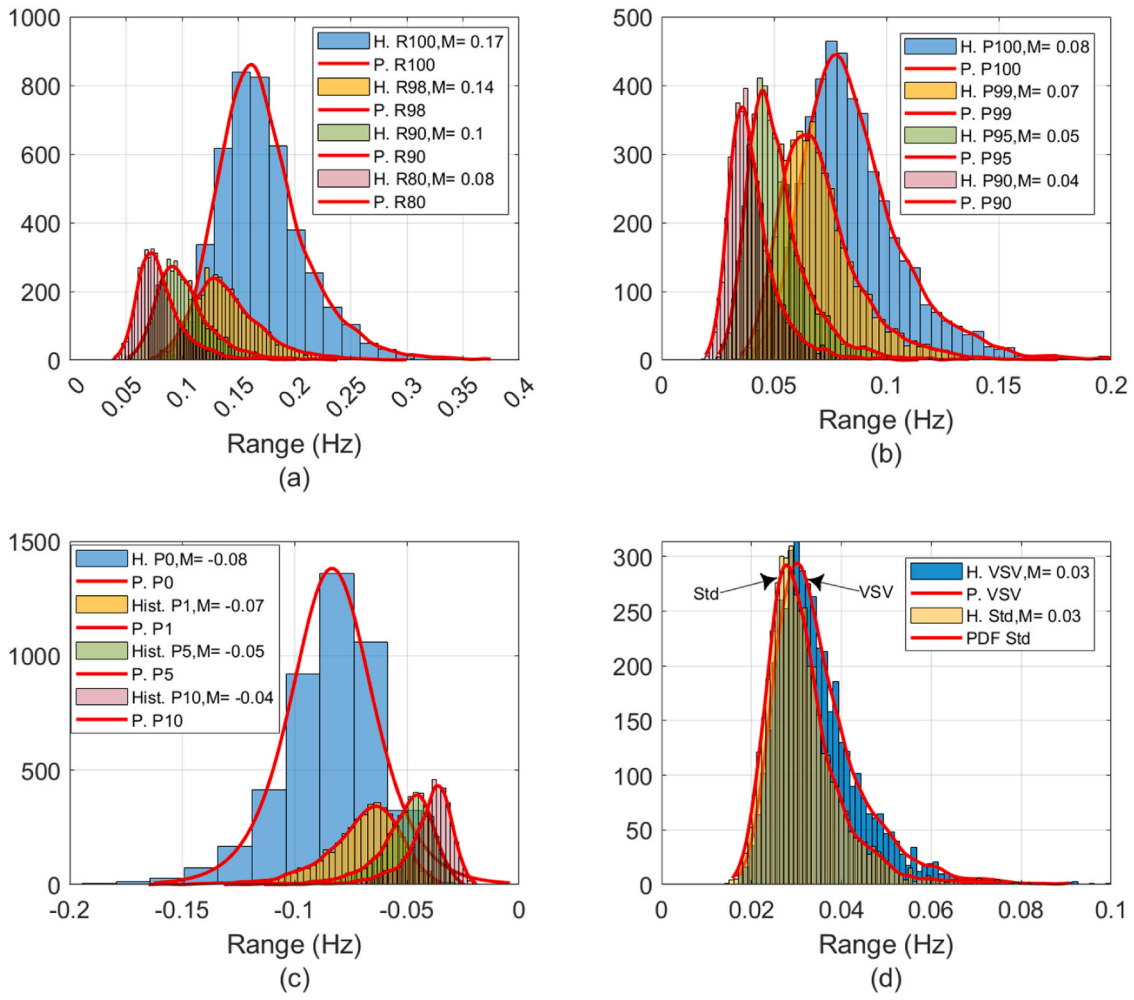

Fig. 6. Histogram fitted by a kernel PDF for the indices quantifying variations as a range in values and VSV within the windows in the input case 1. H: Histogram, P: PDF, M: Median.

Table 3
A comparison between under-deviation and over-deviation indices in input case 1 with a threshold of 0.01 Hz.

Under-deviation higher than over-deviation	P0 > P100	P1 > P99	P5 > P95	P10 > P90
	22.58%	20.24%	8.48%	2.43%
Over-deviation higher than under-deviation	P0 < P100	P1 < P99	P5 < P95	P10 < P90
	26.57%	23.82%	9.51%	2.96%

The SNPNPs, the category of fluctuations, and the number of outliers for the samples shown in Fig. 3 are given in Table 1. The oscillatory level in the samples in Fig. 3 for the input case 1 is from higher to lower for Fig. 3a to Fig. 3g, and Fig. 3d, respectively. No outlier is found in Fig. 3g since the variations deviate around 50 Hz. The CDFs on all the windows in input case 1 for SNPNP and the number of outliers (with three methods) are shown in Figs. 8 and 9.

The CDF for the SNPNP (in % of window length) in Fig. 8 shows that the values for the windows vary from 6% to 35% of window length. 55% of the windows are defined as low fluctuations, 33% as medium, and 12% as high. The quartile method has detected a higher number of outliers per window compared to the others and shows that 38% of windows include at least one outlier for the value 10-s frequency values, while the median method shows 25%, as shown in Fig. 9. According to the mean method, 87% of the windows has no outlier.

4.1.2. Input case 2

The values of the indices R100, P100, P0, and VSV for the samples shown in Fig. 3 are given in Table 1. The histograms for the indices quantifying variations as a range in values and VSV within the windows in input case 2 are shown in Fig. 10. Fig. 10a shows that the frequency deviates by 0.05 Hz to 0.35 Hz within the sub-1-hr windows with 10-s resolution (0.01 Hz higher because of the long window length compared with input case 1). Almost 20%, 9.2%, 9.6%, and 10.6% of the windows have values around the median for R100 (0.17 Hz), R98 (0.14 Hz), R90 (0.1 Hz) and R80 (0.08 Hz). The difference between indices R100 and R80 is 0.09 Hz for the median, and for the 100th percentile is almost 0.2 Hz. These differences confirm the variations happening within the sub-1-hr windows. The cumulative percentage of windows exceeding a 0.2 Hz range is 20%, 5.4%, 0.75%, and 0.02% for R100, R99, R90, and R80, respectively.

Similar to Fig. 6a and b, comparing the results of Fig. 10a and b show a factor of two between the values. The histogram of P0 in Fig. 10c is different from the other under-deviation indices. For example, 30% of the windows have values around the median (-0.08 Hz) from −0.07 to −0.09 Hz. Table 4 shows that the over-deviations more often dominate under-deviations. Moreover, for about 40%, 55%, 90%, and 99% of the windows, the difference between the indices deviates within 0.01 Hz. The VSV values are higher than Std, as shown in Fig. 10d; however, they have a similar value for median as 0.03 Hz.

The number of OF and UF values for the samples shown in Fig. 3 are given in Table 1. NOF indices for Fig. 3h are higher than the other

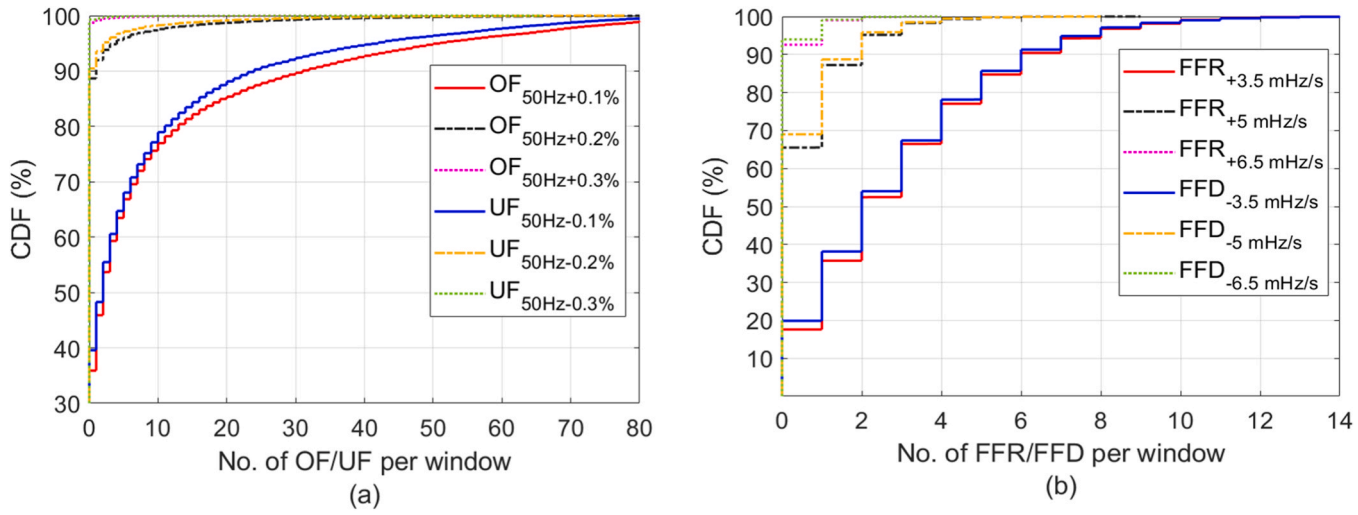

Fig. 7. CDF for the indices quantifying events (except VSV) within the windows in the input case 1. (a) OF/UF; (b) FFD/FFR.

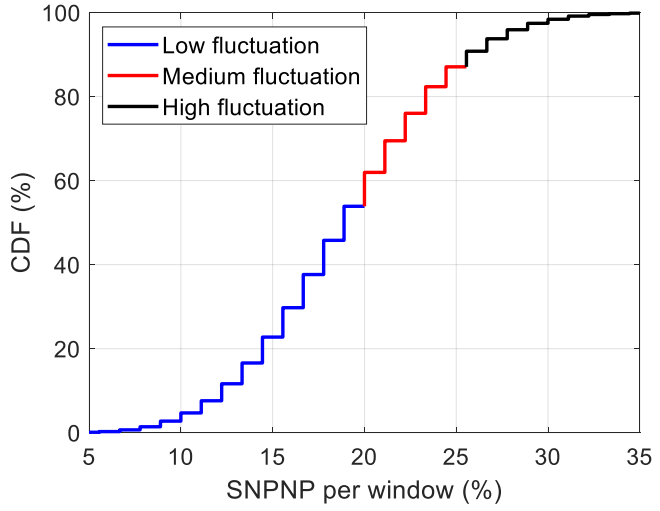

Fig. 8. CDF for the index quantifying the fluctuations within the windows in the input case 1.

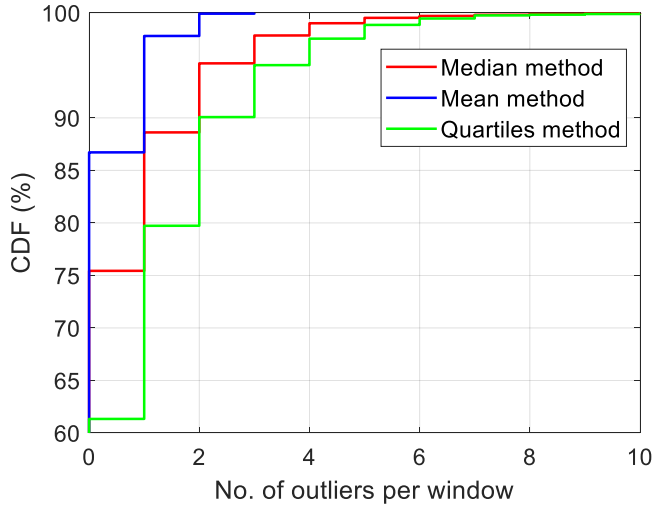

Fig. 9. CDF for the indices quantifying the number of outliers within the windows in the input case 1.

samples (Fig. 2b and e) since the majority of the frequency values are above nominal frequency. A CDF on all the windows in input case 2 is shown in Fig. 11a, which shows that OF/UF values with the threshold 0.1% are more common in terms of occurring within the windows, and almost 32% of the windows have at least 36 times (10% of the window length) OF/UF. About 70% and 95% of the windows have no OF/UF due to the thresholds 0.2% or 0.3%, which shows windows due to NOF2/NUF2 are relatively common, and windows due to NOF3/NUF3 are less common. According to Fig. 11, the NOF1/NUF1 for the windows has varied between 1 and 300 (84% of window length). Similar to Fig. 7a in the input case 1, the NOF1 is higher than NUF1 for the percentiles higher than the median. For example, considering all samples, there is a 49-unit difference, and for the 80th percentile, there is just a 14-unit difference. The NFFR and NFFD for the samples shown in Fig. 3 are given in Table 1, and the CDFs on all the windows are shown in Fig. 11b. FFR/FFD values with the threshold of 3.5 mHz/s are common because almost 80% of the windows has experienced it up to 17 times. The values with the threshold of 5 mHz/s are relatively common since 65% of the windows have at least one, and the values with the threshold of 6.5 mHz/s are less common because almost 80% of the windows have no FFR/FFD. The CDFs for the number of FFD/FFR are very similar, with slightly higher values in FFD.

The SNPNPs, the category of fluctuations, and the number of outliers for the samples shown in Fig. 3 are given in Table 1. The level of oscillatory in the samples in Fig. 3 for the input case 2 is similarly low fluctuation. No outlier is found in Fig. 3 for all three samples according to the median, mean, and quartile methods. The CDFs on all the windows in input case 2 for SNPNP and the number of outliers are shown in Figs. 12 and 13, respectively.

The CDF for the SNPNP shows that the values for the windows vary from 5% to 30% of window length. Almost similar to Fig. 8 for the samples in input case 1, 55% of the windows are defined as low fluctuations, 35% as a medium, and 10% as high. The quartile method has detected a higher number of outliers per window compared to the others and shows that 70% of windows include at least one outlier for the value 10-s frequency values, while the median and mean methods show a 50% and 47%, as shown in Fig. 13.

4.1.3. *Input case 3*

The values for the indices R100, P100, P0, and VSV for the sample windows shown in Fig. 3 are given in Table 1. Fig. 14 shows similar histograms for R100-R98, P100/P99, and/or P0/P1 due to the less window length (m=20) compared to window lengths in input cases 1 and 2. Moreover, the distribution is far away from the normal, so the median values are on the right side of the PDF. It means that the average

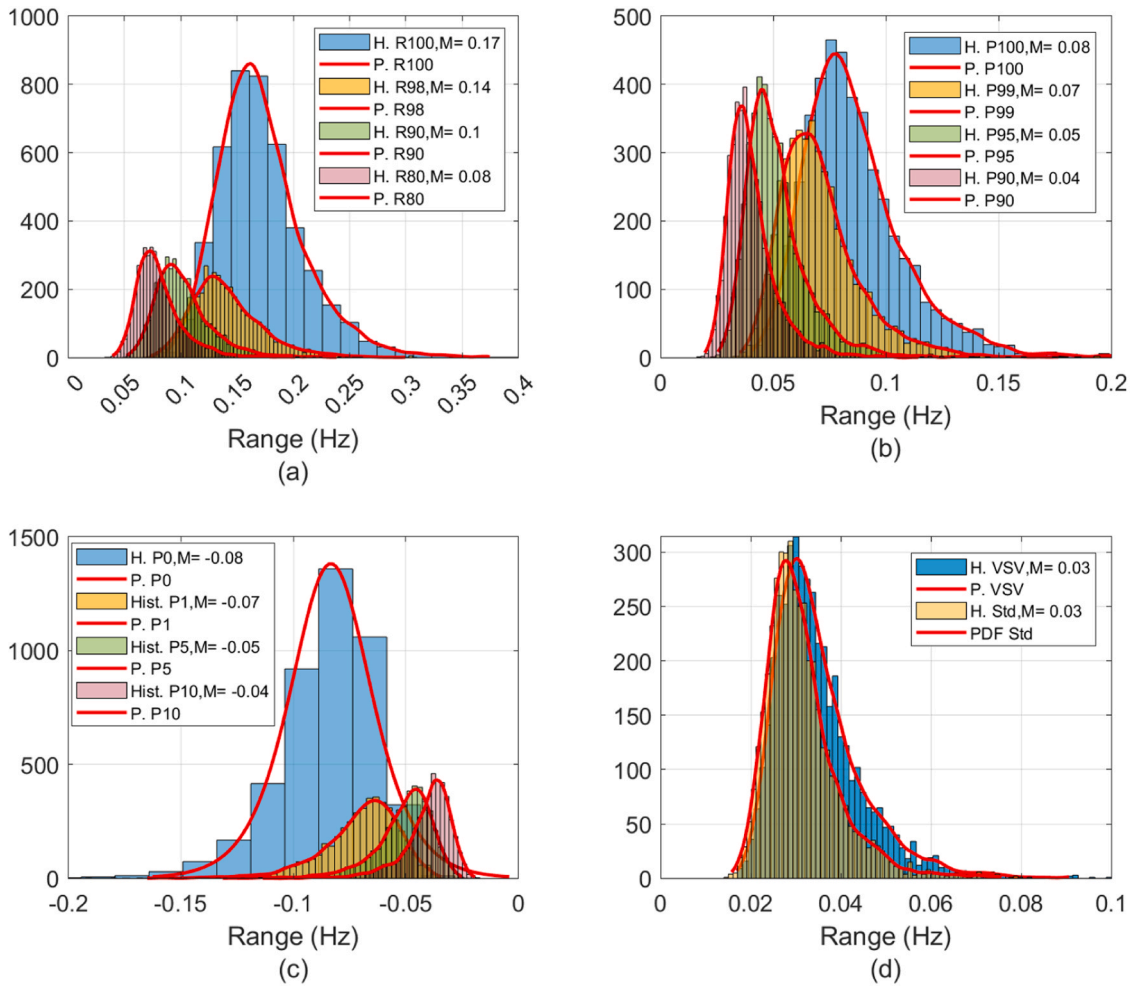

Fig. 10. Histogram fitted by a kernel PDF for the indices quantifying variations as a range in values and VSV within the windows in the input case 2. H: Histogram, P: PDF, M: Median.

Table 4
A comparison between under-deviation and over-deviation indices in input case 2 with a threshold of 0.01 Hz.

Under-deviation higher than over-deviation	P0 > P100	P1 > P99	P5 > P95	P10 > P90
	28.46%	21.22%	8.72%	3.7%
Over-deviation higher than under-deviation	P0 < P100	P1 < P99	P5 < P95	P10 < P90
	31.83%	21.93%	8.97%	3.8%

and median values are different; for example, the median for R100/R98 is about 0.087 Hz (rounded in Fig. 14a as 0.09 Hz), while the average is 0.093 Hz.

The frequency deviates by 0 Hz to 0.25 Hz within the sub-1-hr windows with 3 min resolution (0.01 Hz lower because of the lower time resolution compared with input case 2), as shown in Fig. 14a. Almost 9.7%, 13.5%, and 13.9% of the windows have the values around the median for R100/R98 (0.09 Hz), R90 (0.08 Hz), and R80 (0.06 Hz). The difference between indices R100/R98 and R80 is 0.03 Hz for the median and about 0.033 Hz for the 100th percentile. These almost similar differences show that although the variations are happening within the sub-1-hr windows; however, the ranges are not that much compared with input cases 1 and 2. The cumulative percentage of windows exceeding a 0.2 Hz range is 0.07%, 0.04%, and 0.01% for R100/R99, R90, and R80, respectively, which are low numbers compared to the values in input case 2. Unlike the set of Fig. 6a and b (input case 1), Fig. 10a and b (input case 2), Fig. 14b and c show a factor of 1.6 between the values. Similar to Table 3 (input case 1) and Table 4 (input case 2), Table 5 shows that the over-deviations lead to under-deviations. For about 50% of the windows, the difference in the indices P0-P00 or P1-P99 deviates within 0.01 Hz.

The NOFs and NUFs for the samples shown in Fig. 3 are given in Table 1. The numbers are low compared to the samples from input cases 1 and 2, which is normal because of the 3-min time resolution of the frequency values. A CDF in input case 3 is shown in Fig. 15a, which shows NUF1 values with the threshold 0.1% are more common, so that 45% of the windows have UF1 at least 2 times (10% of the window length). 75%, 88%, 97%, 99.3%, and 99.8% of the windows have no OF/UF for the NOF1 (less common), NUF2, NOF2, NUF3, and NOF3, respectively Fig. 15a also shows that the NOF1 and NUF1 for almost 68% of the windows have varied between 1 and 20 (100% of window length). Unlike Fig. 7a (input case 1) and Fig. 11a (input case 2), the NUF is higher than NOF in Fig. 15a; for example, for the 80th percentile, there is a 6-unit difference. The NFFR and NFFD for the samples shown in Fig. 3 are given in Table 1, and the CDFs on all the windows are plotted in Fig. 15b. FFR/FFD values with a threshold of 10 mHz/min are relatively common because almost 83% of the windows has experienced at least one FFD/FFR. The values with the thresholds 15 and 20 mHz/min are less common since 60% and 85% of the windows have no FFR/FFD. The CDFs for the number of FFD/FFR are very similar (with slightly higher) to the values in FFR.

The SNPNPs, the category of fluctuations, and the number of outliers for the samples in Fig. 3 are given in Table 1. All three samples in Fig. 3

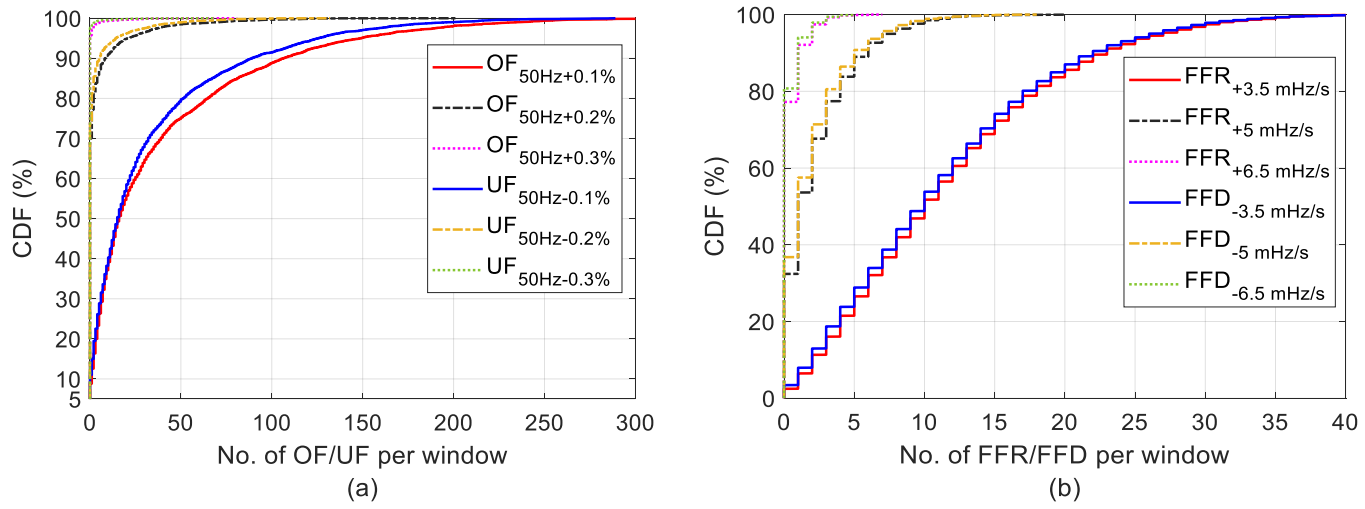

Fig. 11. CDF for the indices quantifying events (except VSV) within the windows in the input case 2. (a) OF/UF; (b) FFD/FFR.

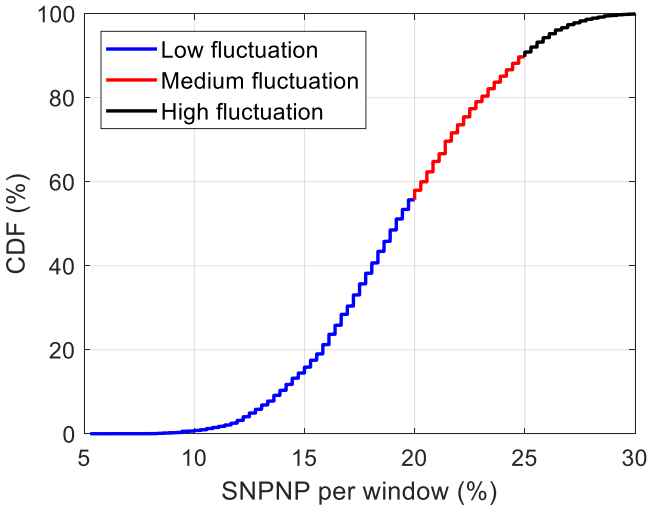

Fig. 12. CDF for the index quantifying the fluctuations within the windows in the input case 2.

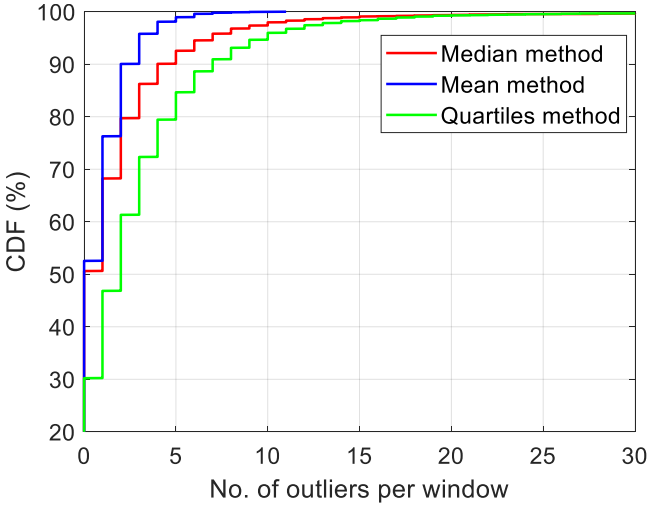

Fig. 13. CDF for the indices quantifying the number of outliers within the windows in the input case 2.

are categorized as low oscillatory. The CDFs on all the windows in input case 3 for SNPNPs in Fig. 16 shows that the values for the windows vary from 5% to 80% of window length. 55% of the windows are defined as low, 41% as medium, and 4% as high fluctuations. The quartile and median methods have detected a higher number of outliers per window compared to the mean method, as shown in Fig. 17; however, the quartile and median methods show only about 22.5% of windows have outliers between 1 and 7 ones.

4.2. *Results of pattern extraction*

In this section, we present the results of the pattern extraction process (Fig. 1) for the three input cases in order to extract the possible patterns that can occur within sub-15-min and sub-1-hr intervals to gain deeper understanding of the frequency variations and fluctuations that take place within these brief time windows (Figs. 18–26). A preliminary examination was conducted on the three input cases. Each window is assigned a specific label based on various criteria, such as: belonging to different months, weekdays or weekends, and different time intervals (e.g., 12–6 am for night-morning, 6 am-12 pm for morning-noon, 12–6 pm for noon-evening, and 6 pm-12 am for evening-night). While these criteria, along with averaging the samples that share similar labels, allowed us to identify certain patterns, there are likely hidden patterns that require further exploration through learning methods. Subsequently, clustering techniques are employed to further analyze the frequency windows. Multiple attempts are made, testing different numbers of clusters, until meaningful insights that align with the physical reality (mostly derived from our pre-labeling manner) are obtained. For input cases 1 and 2, a consistent choice of 6 clusters is made, while input case 3 is determined to have 7 clusters due to a longer data period. It is observed that increasing the number of clusters beyond these values resulted in subdivisions that lacked significance or meaningful interpretation. The squared Euclidean distance measurement (as the most famous one) is used for the clustering techniques. The t-SNE parameters (in Fig. 3) are as Barnes hut algorithm, Euclidean distance, perplexity=30, and maximum iteration=100 for all input cases, and the number of used PCA components is 25, 50 and 0 for the input cases, respectively). The parameters for clustering techniques and t-SNE are selected to produce meaningful patterns and well-separated clusters. Since t-SNE shrinks widespread data and expands densely packed data, it is not reasonable to decide the size of clusters on t-SNE plots; hence, the size of clusters (C1, C2, …) is given further for each cluster separately. Note that the overlap seen in t-SNE plots is due to plotting high-dimensional feature vectors into only two dimensions; however, the clustering is soft, and each sample belongs to one cluster. The centroids

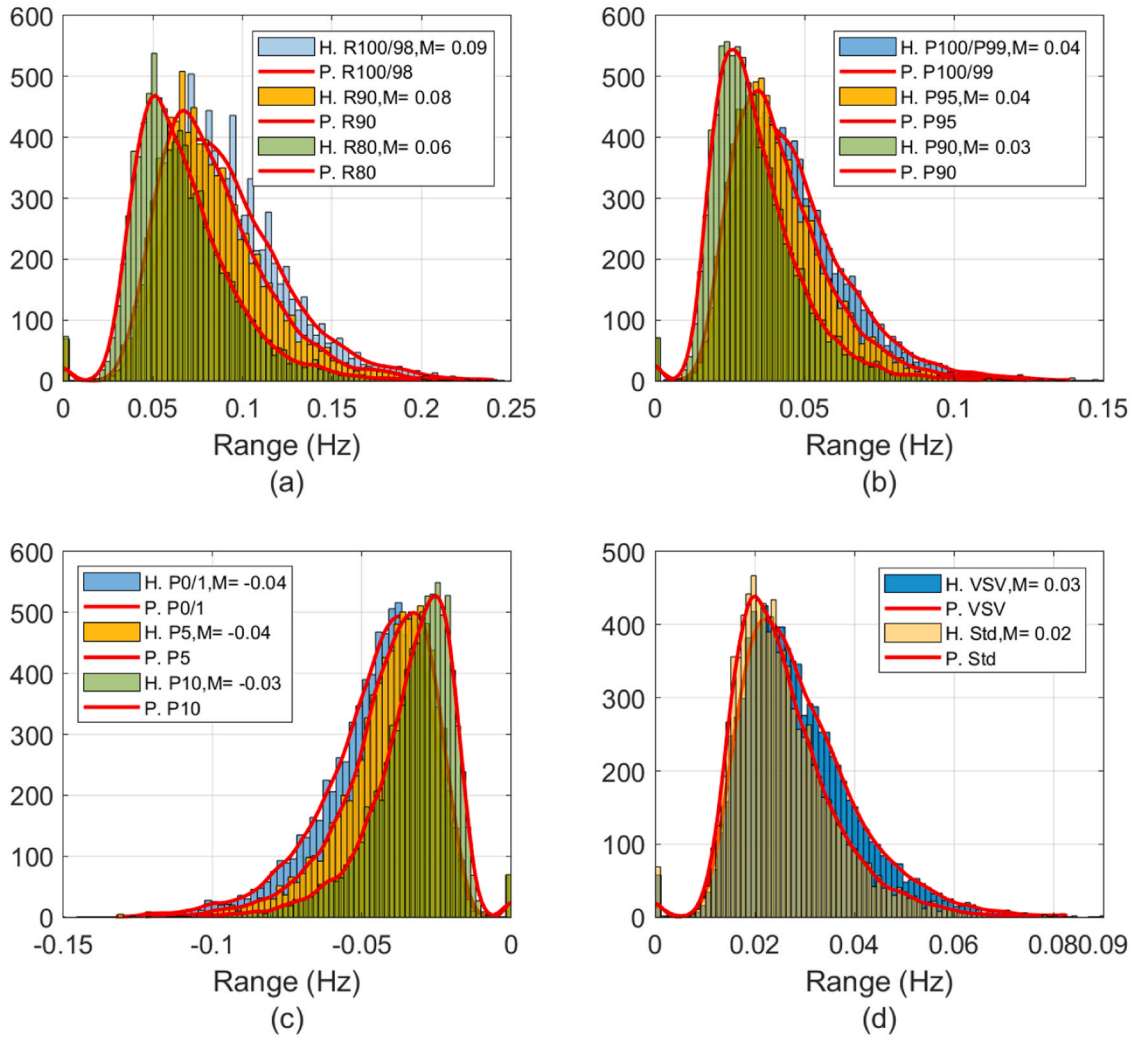

Fig. 14. Histogram fitted by a kernel PDF for the indices quantifying variations as a range in values and VSV within the windows in the input case 3. H: Histogram, P: PDF, M: Median.

Table 5
A comparison between under-deviation and over-deviation indices, in input case 3, with a threshold of 0.01 Hz.

Under-deviation higher than over-deviation	P0>P100 or P1>P99	P5>P95	P10>P90
	23.29%	17.76%	10.98%
Over-deviation higher than under-deviation	P0<P100	P5<P95	P10<P90
	27.36%	20.94%	12.47%

(Ctds)/medoids (Mdds) as the cluster centers are also marked by ×.

4.2.1. Input case 1

By analyzing the results of t-SNE (Fig. 18) and extracted sub-15-min patterns (Figs. 19 and 20, in which the number of samples belonging to each cluster is written on the top of sub-figures), the following observations regarding six typical patterns can be made:

1. According to the pre-discovery of the dataset (explained in 4.2), patterns P_6^{kmn}/P_3^{kmd} can be representative of the frequency variations in sub-15-min for the whole included months (except July) in the period of the evening – night. Patterns $P_4^{kmn}/P_2^{kmd}/P_3^{kmd}$ could be regarding July for that period of day and night.
2. Patterns P_3^{kmn}/P_4^{kmd} can represent the frequency variations for the whole included months in the periods of the morning – noon and/or noon – evening. These patterns are the more common patterns seen in the frequency variation in sub-15-min windows.
3. Patterns P_2^{kmn}/P_6^{kmd} could show the behavior of sub-15-min windows for the whole included months (except July) in the period of the night – morning, in which the range of frequency variations is less than the other parts of day night. Patterns P_5^{kmn}/P_5^{kmd} were much more observed in July for that period of day and night.
4. The downward pattern P_1^{kmn}/P_1^{kmd} is the pattern that was not realized during our pre-processing; however, the clustering techniques could extract it, and there might be a physical reality linked to the sub-15-min windows.
5. Looking at the sub-15-min patterns extracted from k-means/k-medoids shows that some behaviors are more visible: sudden drops in 10-s values (almost in all patterns), sudden rises in 10-s values (almost in all patterns), the slow drift of 10-s values mainly towards a high value over the window with variations in between ($P_4^{kmn}/P_6^{kmn}/P_3^{kmd}$), the slow drift of 10-s values towards a low value over the window with variations in between ($P_1^{kmn}/P_5^{kmn}/P_1^{kmd}/P_5^{kmd}$), U-shape variations' pattern as seen in P_2^{kmn} and fluctuations in frequency 10-s values ($P_3^{kmn}/P_2^{kmd}/P_4^{kmd}$).
6. Although Fig. 18a shows a better cluster separation for k-means compared with k-medoids (Fig. 18b); however, the extracted patterns (Figs. 19 and 20) state that there is not much more difference between them in terms of the shape of variations. The visible difference is the range-wider variations in k-medoids' patterns because

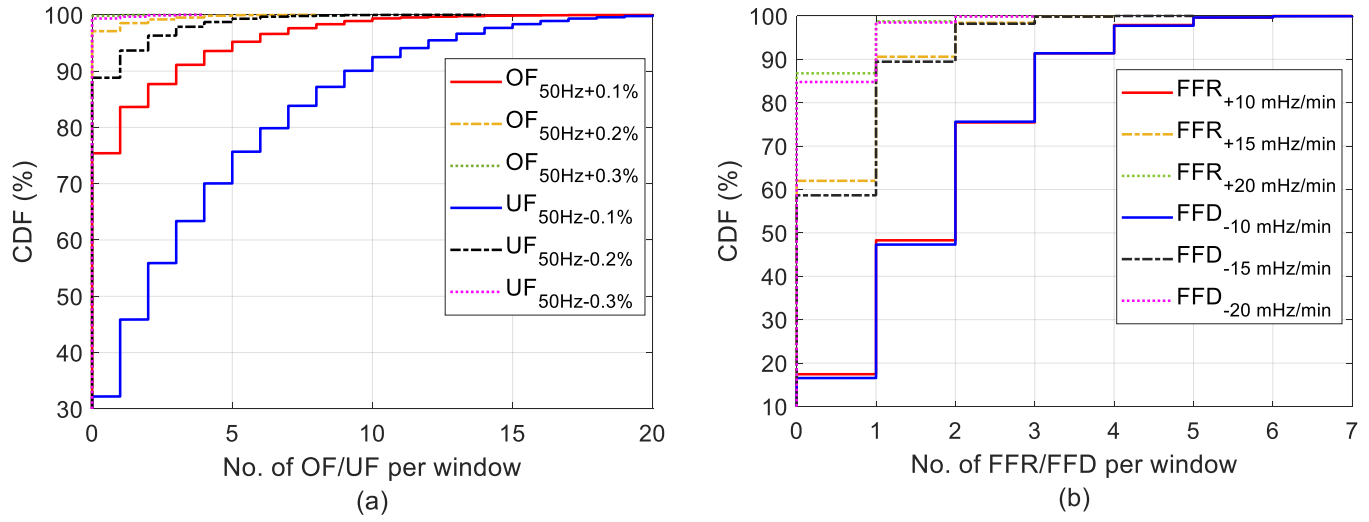

Fig. 15. CDF for the indices quantifying events (except VSV) within the windows in the input case 3. (a) OF/UF; (b) FFD/FFR.

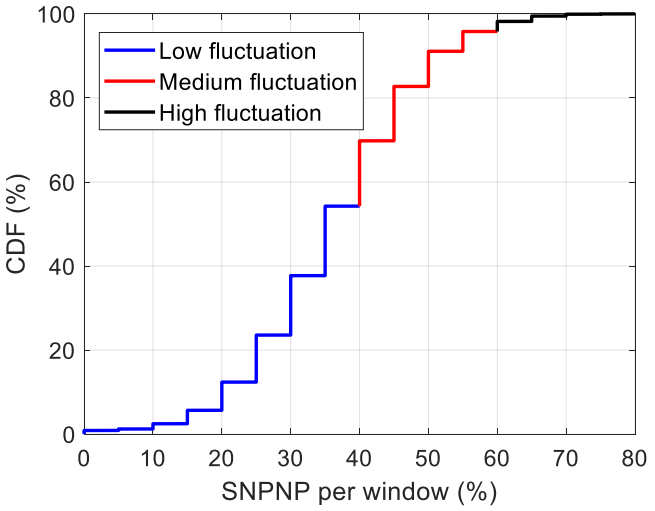

Fig. 16. CDF for the index quantifying the fluctuations within the windows in the input case 3.

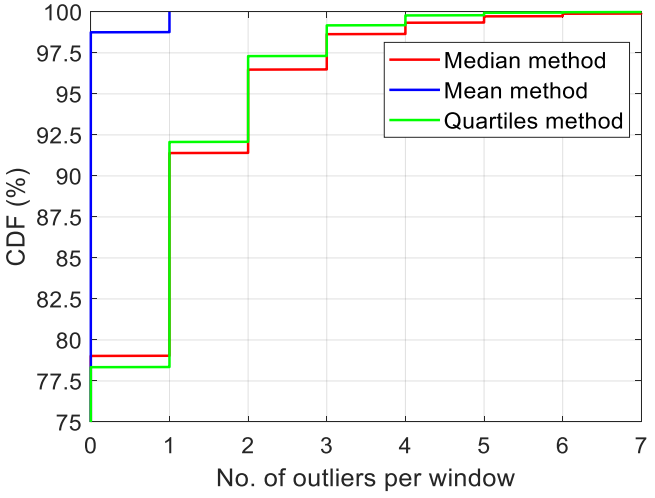

Fig. 17. CDF for the indices quantifying the number of outliers within the windows in the input case 3.

each pattern is a real input sample (window) from matrix *X* and not an average of samples within a cluster, as extracted from k-means.

4.2.2. *Input case 2*

By analyzing the results of t-SNE (Fig. 21) and extracted sub-1-hr patterns (Figs. 22 and 23), the following observations regarding six typical patterns can be made:

1. Patterns $P_1^{kmn}/P_2^{kmn}/P_2^{kmd}$ can represent the frequency variations for the whole included months (except July and August) in the period of the evening – night. Pattern P_1^{kmd} was seen more in July and August during that period of day and night.
2. The behavior of windows belonging to the morning-noon period in July and August was more observed in the patterns P_5^{kmn}/P_3^{kmd}.
3. Pattern P_5^{kmd} could show the behavior of windows for the whole included months (except July) in the period of nigh – morning, in which the range of frequency variations is less than the other parts of day and night. Patterns P_1^{kmn} and P_6^{kmn} were seen more in July and March, respectively, for that period of day and night.
4. The rest of the patterns, $P_3^{kmn}/P_4^{kmn}/P_4^{kmd}/P_6^{kmd}$, show some existing downward patterns in which a physical reality could be linked with that for the sub-1-hr windows.
5. Looking at the sub-1-hr patterns shows that some behaviors: sudden drops/rises in 10-s values (almost in all patterns but less visible compared to sub-15-min windows in the input case 1, 4.2.1), slow mainly increasing trend in the 10-s values with some possible different behavior at first/last 20 min of the windows ($P_1^{kmn}/P_2^{kmn}/P_1^{kmd}/P_2^{kmd}$), slow mainly decreasing trend in values with some possible different behavior at first/last 20 min of the windows ($P_3^{kmn}/P_4^{kmn}/P_3^{kmd}/P_4^{kmd}$), and fluctuations in frequency 10-s values ($P_4^{kmn}/P_6^{kmn}/P_5^{kmd}/P_6^{kmd}$).
6. Similar to the results of sub-15-min windows in 4.2.1, although Fig. 21a shows the well-distinguished clusters for k-means (slightly better); however, the extracted patterns (Figs. 22 and 23) state the much similar patterns in the shape of variations, but with wider ranges for the k-medoids' patterns.

Compared with sub-15-min windows (4.2.1), the sub-1-hr patterns show more complex behaviors in the variations because of the bigger window length. The last 20-min in P_2^{kmn}/P_2^{kmn} and the first 20-min in $P_1^{kmn}/P_3^{kmn}/P_1^{kmd}$ are seen as some fluctuations, and the fluctuations with a trend to an up value are seen in P_5^{kmn}/P_3^{kmd}.

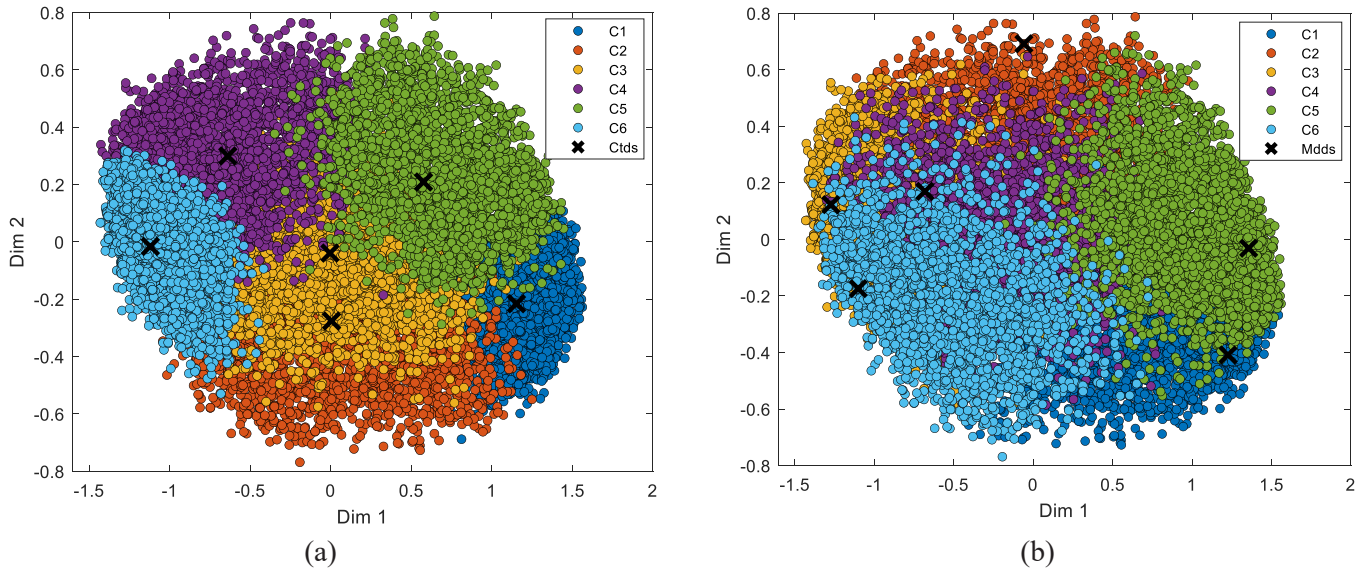

Fig. 18. Visualization of 90D clustered input vectors into 2D for input case 1 using via clustering techniques (a) K-means; (b) K-medoids.

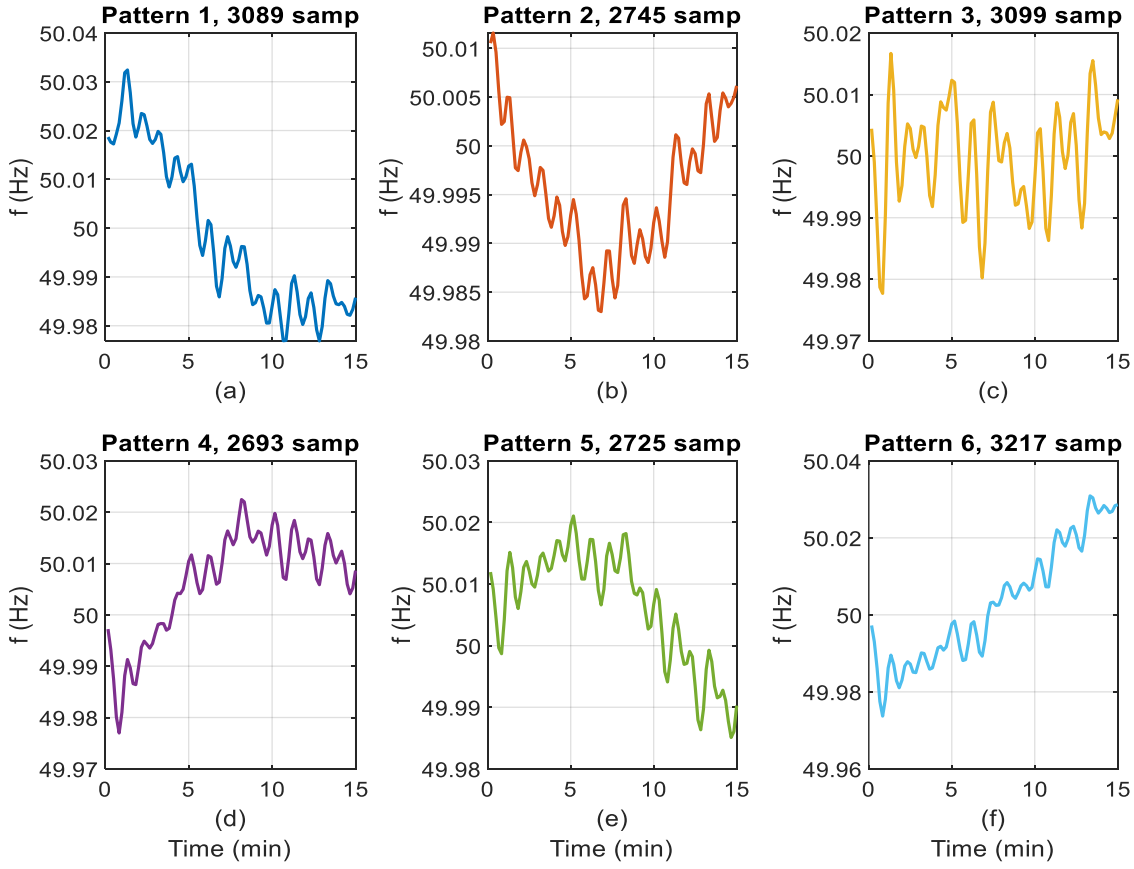

Fig. 19. Extracted sub-15-min patterns from k-means for the input case 1.

4.2.3. *Input case 3*

The idea for the pattern extraction from the sub-1-hr windows with the 3-min resolution is to seek whether there are any different existing possible patterns for the entire year (in our case 2021) compared to the sub-1-hr windows with 10-s resolution (Input case 2). Firstly, it is worth noting that the overlapping of clusters 1 and 6 (shown in Fig. 24a), as well as clusters 4 and 6 (shown in Fig. 24b), results from the 20D feature vectors being visualized in just two dimensions. However, visualizing the data in a 3D plot made it clear that the overlapped clusters are actually situated in opposite directions on a sphere. Additionally, the results in Figs. 25 and 26 show that the patterns for input case 3 somehow have a smoothed average of the patterns for input case 2 because they have a bigger time resolution. The only extra pattern is $P_1^{kmn}/P_6^{kmd,}$ in which the downward/upward trends are being changed during each 20 min.

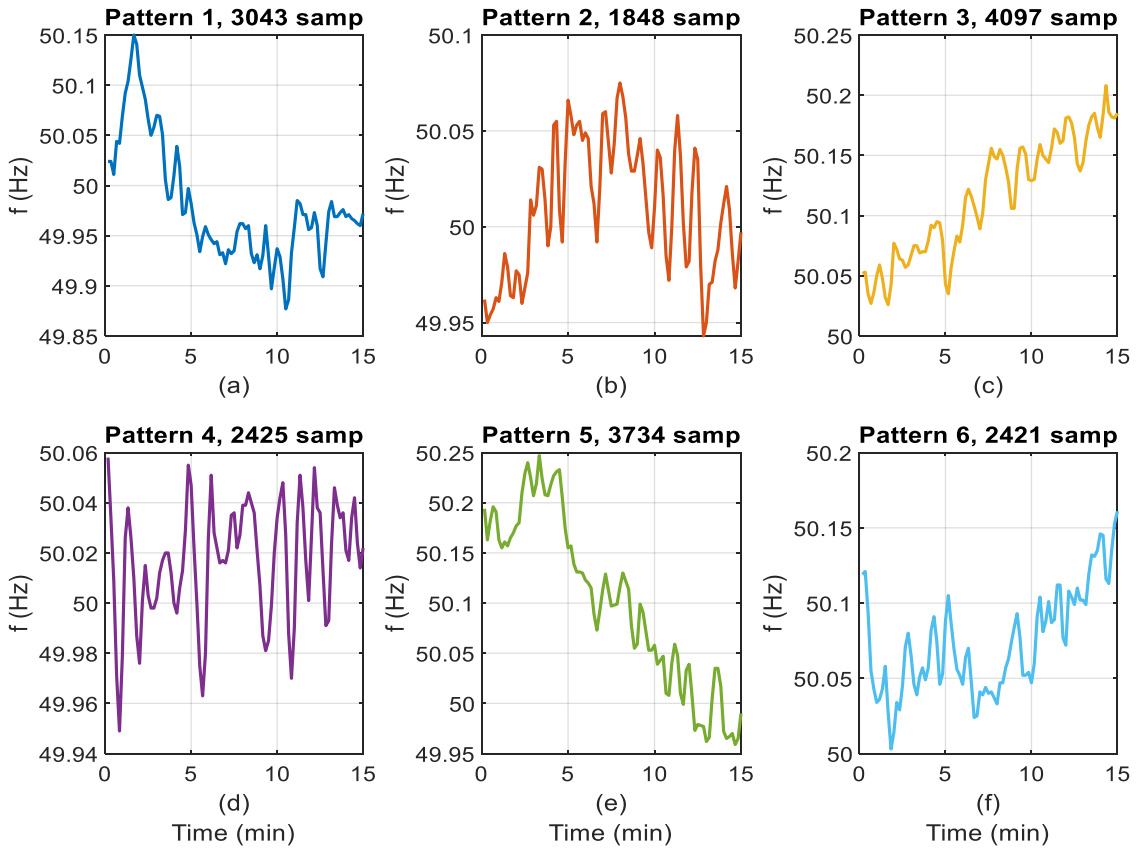

Fig. 20. Extracted sub-15-min patterns from k-medoids for the input case 1.

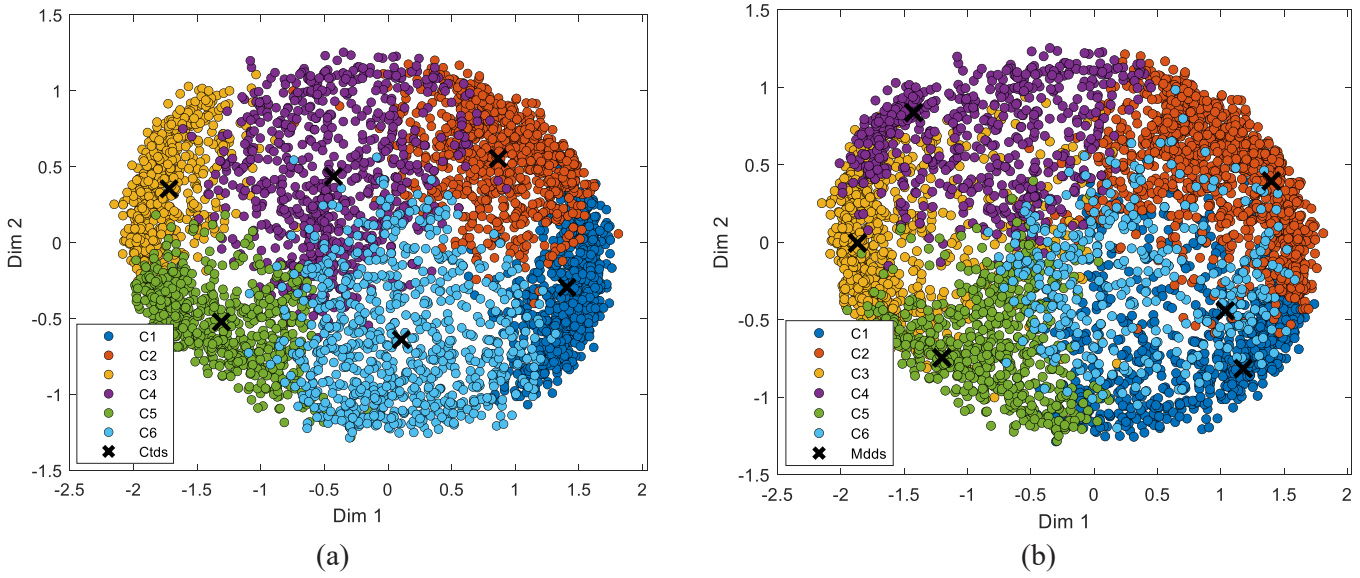

Fig. 21. Visualization of 360D clustered input vectors into 2D for the input case 2 via clustering techniques (a) K-means; (b) K-medoids.

Table 6 gives the obtained patterns for the samples shown in Fig. 3. As seen in this table, the patterns follow the real samples for each of the three input cases.

4.2.4. *Summary of pattern extraction findings*

A summary of the findings from the frequency pattern analysis conducted on the input cases regarding short time scales are explained as follows:

1. Around 6 or 7 "typical patterns" were identified within the short time scales of frequency values, regardless of the window lengths and the period of study.
2. In cases where the short time scales have higher time resolutions, typically within a few seconds, the extracted patterns demonstrate the ability to detect and illustrate sudden drops effectively or rises in frequency.

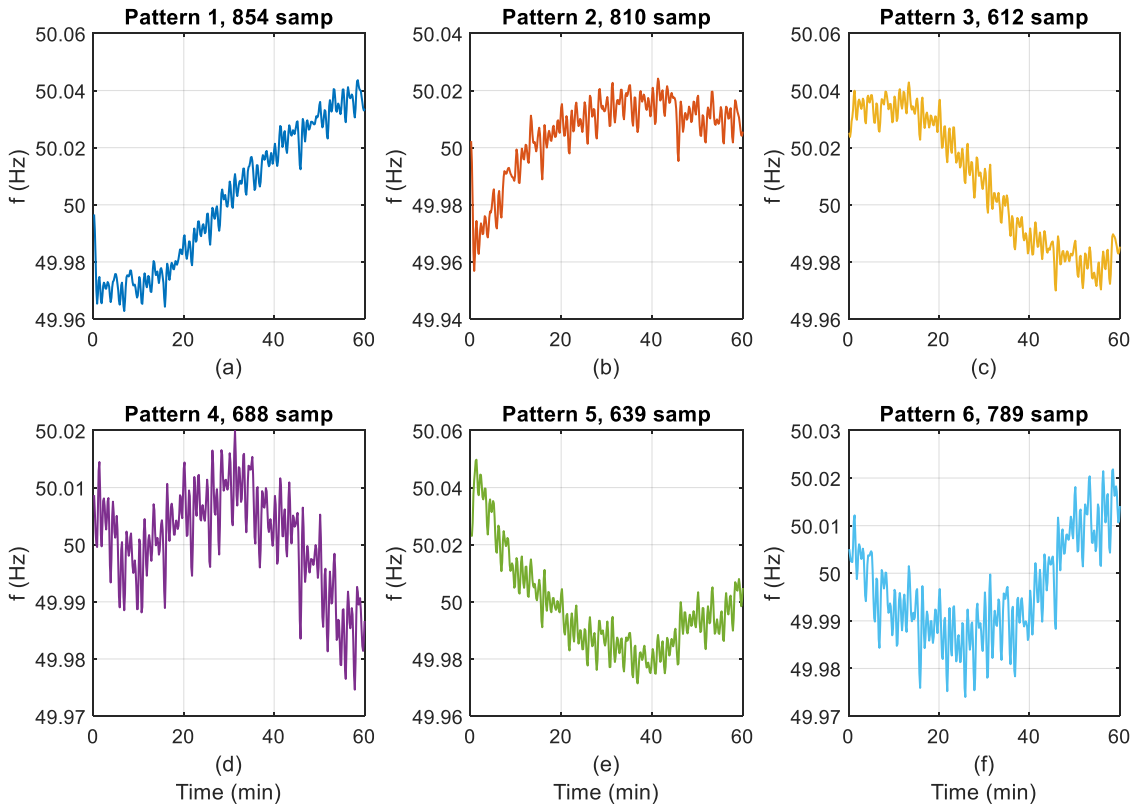

Fig. 22. Extracted sub-1-hr patterns from k-means for input case 2.

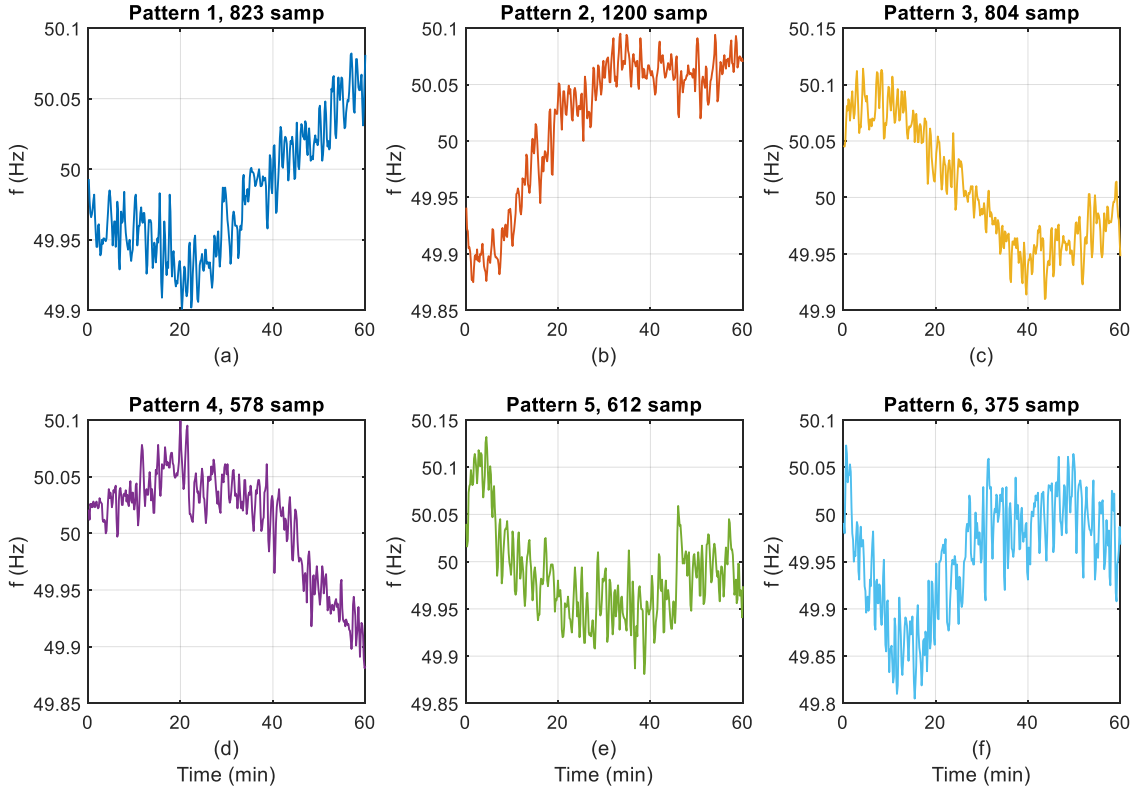

Fig. 23. Extracted sub-1-hr patterns from k-medoids for the input case 2.

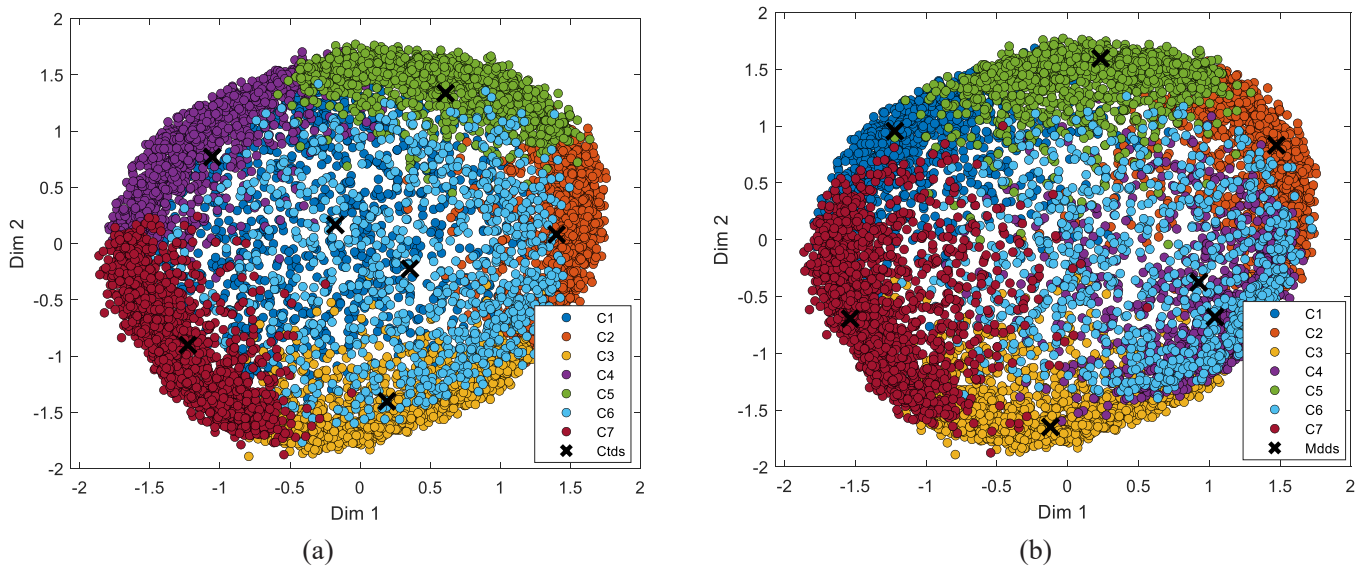

Fig. 24. Visualization of 20D clustered input vectors into 2D for input case 3 via clustering techniques (a) K-means; (b) K-medoids.

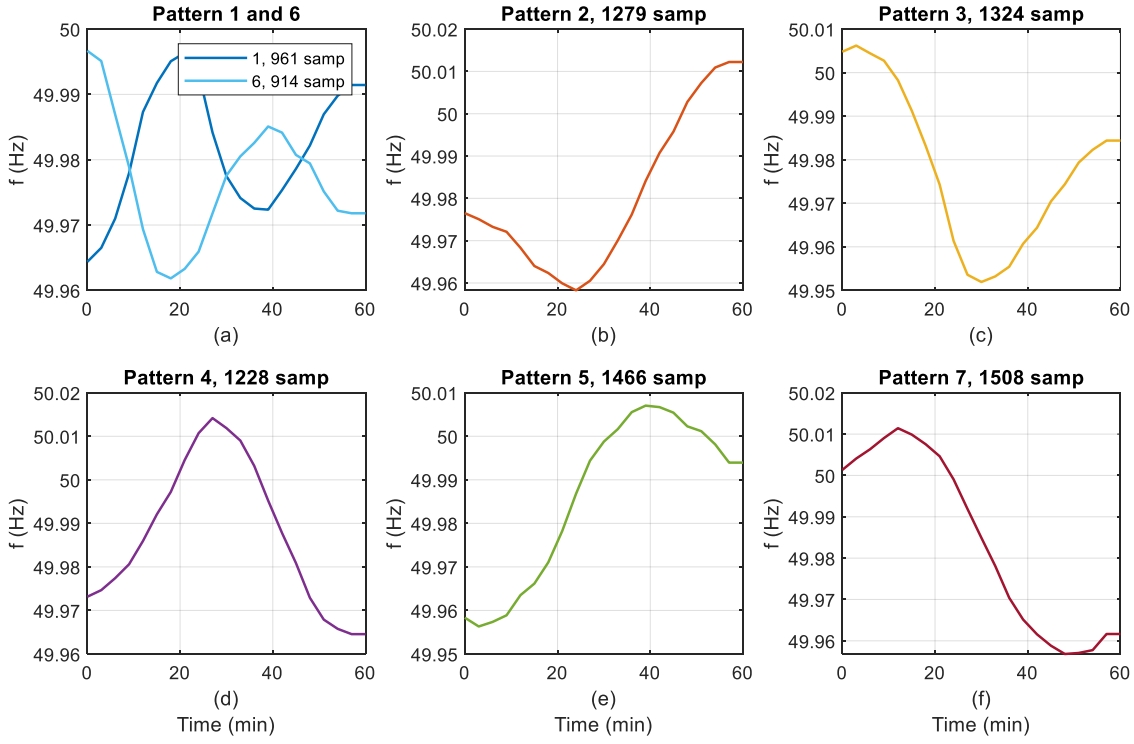

Fig. 25. Extracted sub-1-hr patterns from k-means for the input case 3.

3. Most of the extracted patterns within the short time scales were consistent with the realities discovered through pre-knowledge labeling. However, the downward patterns were specifically obtained by considering particular window lengths.
4. By utilizing the extracted patterns within the short time scales, each frequency window can be assigned to a specific pattern from the 6 or 7 identified patterns. This enables easier analysis of the extensive dataset of frequency instants, called big data analysis, through these pattern-based frequency windows, facilitating future frequency control design and planning objectives.
5. As frequency instants or trends can be influenced by various factors such as generation ramping, market dynamics, and flexible grid operations, monitoring the pattern-based windows can provide valuable insights for network operators. By analyzing these windows, operators can gain an understanding of the performance of controllers, as well as the impact of market activities and flexible grid operations on the frequency patterns. This information is crucial for assessing the overall system stability, optimizing control strategies, and making informed decisions regarding market and grid operations.

5. Discussion

5.1. Identifying the most significant statistical indices

In total, 36 statistical indices were considered in this study in which 13 indices were “proposed” as indices quantifying the events and

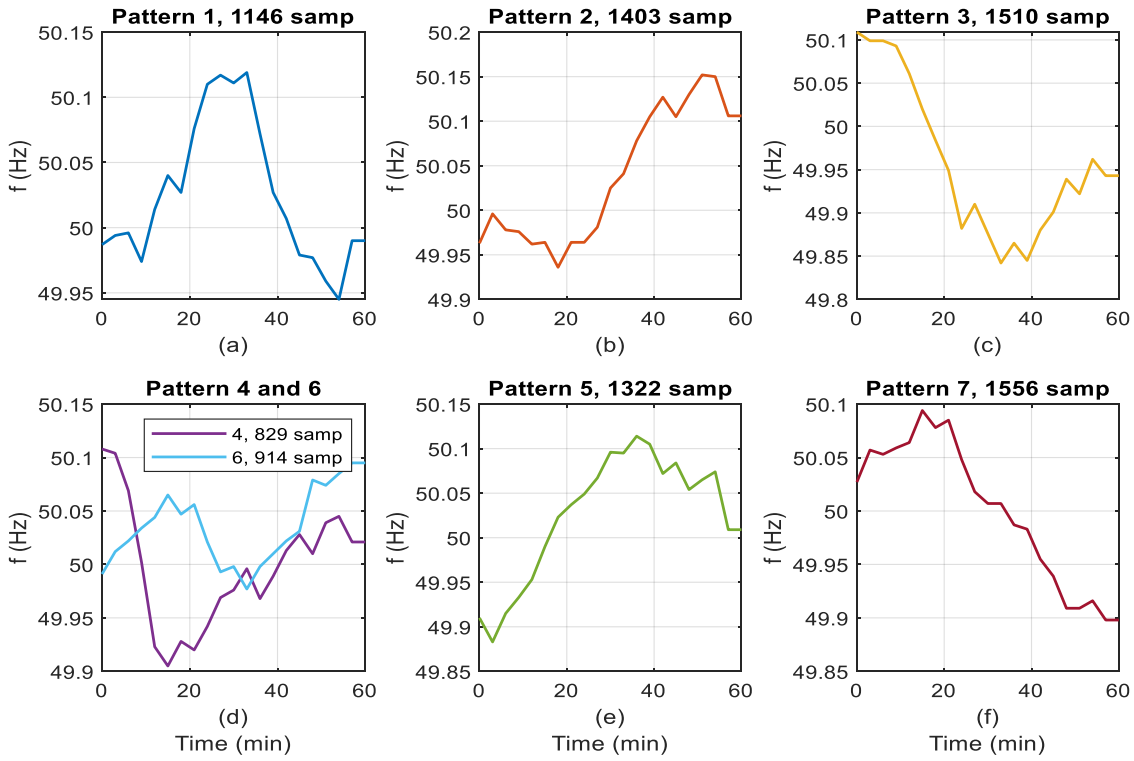

Fig. 26. Extracted sub-1-hr patterns from k-medoids for the input case 3.

Table 6
The extracted patterns assigned to the samples shown in Fig. 3.

Clustering method	Input case 1			Input case 2			Input case 3		
	(a)	(d)	(g)	(b)	(e)	(h)	(c)	(f)	(i)
K-means	1	6	2	1	6	3	2	3	4
K-medoids	1	3	4	2	4	3	2	3	1

fluctuations, i.e., NOF (3 indices), NUF (3 indices), NFFR (3 indices), NFFD (3 indices), and SNPNP (1 index). Furthermore, 13 additional indices proposed in [29] were used and applied to the frequency values in this study as R and P indices along with VSV. In addition, 10 more well-known indices were applied to the frequency values as Mean, Max, Min of *f*/RoCoF, Std, and Noutliers.

In practice, and according to the results concluded from this study, there may be no need to use all indices. Hence, identifying the most significant indices can save computational expense. For the indices quantifying the ranges (except Std.), in a similar way to our previous works [44,45], the most dominant index is selected as "*the one that has the strongest (maximum) correlation with the other indices in each set*". First, the correlation matrix of each set is calculated, and then an average is taken between the correlation coefficients of each index and the others. Finally, the maximum between all averaged coefficient values is selected. Generally, "36 initial indices" are turned into a maximum "15 dominant ones", as follows:

- The mean index is chosen from the set (Mean, Max, Min of *f*/RoCoF) for all input cases (2 dominant indices). R98, R98/R90, and R90 are chosen from the set (R100, R98, R90, R80) for input cases 1, 2, and 3, respectively (1 or 2 dominant indices).
- P99, P99/P95, and P95 are chosen from the set (P100, P99, P95, P90) for input cases 1, 2, and 3, respectively (1 or 2 dominant indices).
- P1, P1/P5, and P5 are chosen from the set (P0, P1, P5, P10) for input cases 1, 2, and 3, respectively (1 or 2 dominant indices).
- Among the VSV and Std., VSV can be selected since it also includes information from the previous window compared to Std. However, between Std. and the Mean of the frequency (*f*), Std. can be selected because of calculating deviations of frequency values from the mean (1 dominant index).
- SNPNP is the only index proposed to quantify the fluctuations (1 dominant index).
- For the indices quantifying the events (except VSV), according to the results obtained from this study, the ones with the biggest thresholds can be selected, i.e., NOF1, NUF1, NFFR1, and NFFD1 (4 dominant indices).

Noutlier3, which uses the quartile method, is chosen among the indices quantifying the outliers since it has detected a greater number of outliers (1 dominant index).

5.2. *Compressing and converting windows using the statistical indices and extracted patterns*

Each statistical index suggested in this paper is a criterion to show the severity of the belongings happening in the windows with sub-15-min and sub-1-hr variations. Compressing 90 (window length in input case 1) and 360 (window length in input case 2) frequency values into smaller statistical indices can reduce the data size needed later in frequency analysis. According to 5.1, from the 13 proposed indices, 5 ones can be selected as dominant ones, i.e., SNPNP, NOF1, NUF1, NFFR1, and NFFD1 (From the outcomes of this study, Noutlier3 is also chosen as a dominant index among the Noutlier1 and 2).

In this way, the compressing factor is 90/6 (15 for input case 1 windows) and 360/6 (60 for input case 2 windows). We must also consider that the indices quantifying the events with trigger mechanism are recorded only when the indices exceed the thresholds; hence, a window may not always need such indices.

Using extracted patterns for the three input cases can convert each of the sub-15-min and sub-1-hr windows to the corresponding pattern for the input cases, i.e., (P_1-P_6 in input case 1, P_1-P_6 in input case 2, and P_1-

P_7 in input case 3). In this way, 17568, 4392, and 8680 windows are converted by repeating only 6 and 7 pattern-sampled windows in input cases 1, 2, and 3, respectively.

5.3. Choosing indices, window lengths, time resolutions, input case studies, and thresholds

Indices instead of aggregated values: Currently, frequency variations are typically identified by aggregating values over a window with a fixed length, such as 5 min, 15 min, 30 min, and 1 hour. Instead of aggregated values at the end of each window, this paper introduces specific statistical proper indices to quantify the variations within the sub-15-min and sub-1-he windows, providing a detailed picture of existing variations. Employing these new indices per window can also improve and revise the grid codes.

Window lengths: The selection of the 15 min and 1 hr window lengths was due to two factors. Firstly, "15-min window intervals" are widely used in European synchronous areas to record frequency measurements for electricity power markets and evaluate frequency control performance. Additionally, article 127 in [1] specifies that it takes 15 minutes to restore the frequency within the standard range (±0.1 Hz) after it deviates from the normal operation. The choice of a "1-hr window length" was made with future considerations in mind, as electricity power market policymakers are starting to transition to 1-hr intervals [25–27]. This longer window length allows for comparing frequency quality and typical patterns with smaller time windows, highlighting any differences.

Time-resolutions: In order to have a full picture and knowledge from the short time-windows, a higher time resolution can introduce more information regarding variations, events, fluctuations, outliers, and typical existing patterns (trends). For example, a maximum or minimum value of lower resolution frequency values might be less than the higher-resolution frequency values, missing some information. Additionally, the extracted patterns while having higher resolution values are more realistic showing the trends within windows including possible variations and oscillations.

Higher-resolution, in this study 10-s values, was selected according to the best available time resolution of the used power-quality device, and 3 min, as lower-resolution, was forced by the available data in [60]. Three input cases were identified as suitable for quantifying frequency quality and capturing typical patterns based on the existing time resolutions and selected window lengths.

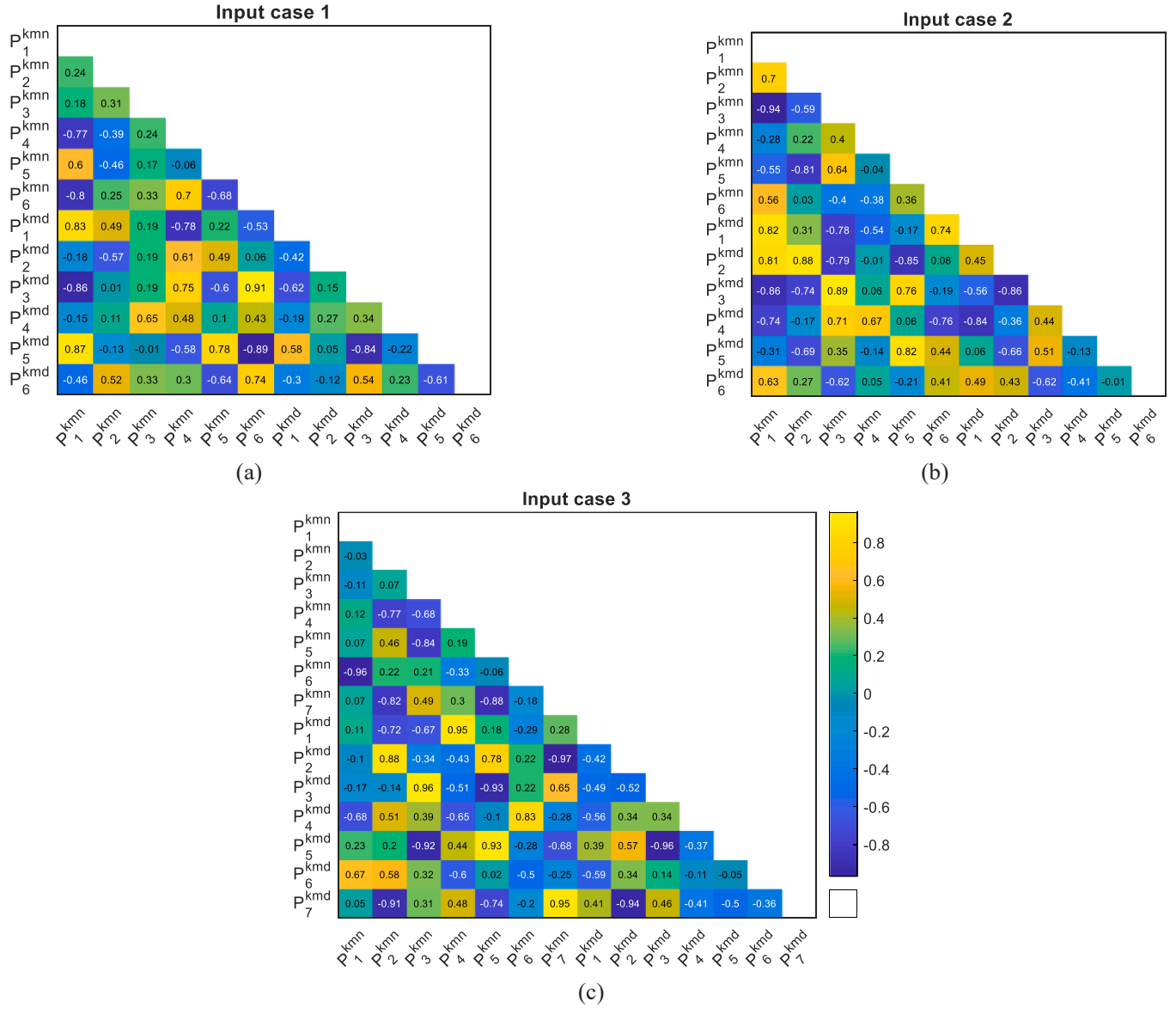

Fig. 27. Correlations between patterns extracted from k-means, k-medoids, and k-means vs. k-medoids for (a) Input case 1; (b) Input case 2; (c) Input case 3.

As explained in 2.1, input cases 1 and 2 are considered to explore variations, events, fluctuations, outliers and typical patterns that may occur in "higher-resolution" frequency values within sub-15-min and sub-1-hr intervals for selected months. Both cases 1 and 2 include 10-s similar frequency values, cover a similar six-month time period, and utilize different short window lengths. Input case 3 comprises different frequency values compared to cases 1 and 2, representing 3-min instants and using 1-hr window lengths similar to case 2. This case serves as a representative example to demonstrate the types of variations and patterns expected in frequency values within sub-1-hr intervals for the entire year 2021, which differs from cases 1 and 2.

Thresholds: The thresholds for NFFR and NFFD were selected based on the RoCoF values calculated for the available time resolutions in input cases 1–3. This selection aimed to provide a meaningful range of the sudden events covered within the windows. Similarly, the 0.01% threshold in the SNPNP was chosen based on the available time resolutions in the input cases 1–3 to show the fluctuations clearly. Although one may use different time resolutions and thresholds for NFFR, NFFD, and SNPNP, this study aims to demonstrate how these indices can be employed as frequency-quality indicators within a specified window length with the existing time resolutions.

5.4. Correlation between extracted patterns

Fig. 27 presents the Pearson correlation coefficients for three different scenarios: between the patterns extracted from k-means (P^{kmn}), between the patterns extracted from k-medoid (P^{kmd}), and between P^{kmn} and P^{kmd}. These correlations are shown for all three input cases (1, 2, and 3) in Fig. 27a, b, and c, respectively. The corresponding patterns can be found in Figs. 19 and 20 (for case 1), Figs. 22 and 23 (for case 2), and Figs. 25 and 26 (for case 3). The correlation coefficients between P^{kmn} itself or P^{kmd} itself are generally in an acceptable range with low values (high positive correlations mean strong similarity), although a +0.7 is seen between P_2^{kmn} and P_4^{kmn} (Input case 1, Fig. 27a) or between P_1^{kmn} and P_2^{kmn} (Input case 2, Fig. 27b). It means there is a well-separation between the frequency windows grouped into the clusters. On the other hand, there are high positive correlations between most patterns of P^{kmn} versus P^{kmd} for all the input cases. For example, the maximum correlations are seen between P_3^{kmd} and P_6^{kmn} for input case 1 and between P_3^{kmd} and P_3^{kmn} for input cases 2 and 3 (Fig. 27b and c). This means that the two clustering methods have somehow extracted similar patterns regarding the shape of variations. However, as shown in Section 4.4, the k-medoids patterns show variations with higher magnitudes or fluctuation ranges. The strong negative correlation (-0.91) between P_1^{kmn} and P_6^{kmn} (as seen in Fig. 27c), which serve as cluster centers for the overlapped clusters 1 and 6 (as seen in Fig. 24a), indicates a clear separation between these two clusters. The almost 180-degree difference in angle between P_1^{kmn} and P_6^{kmn} in a 2D space (the patterns are marked by the × in Fig. 24a) serves as additional evidence for their high negative correlation approaching −1.

5.5. Comparison between the input cases

a. *In terms of the statistical indices*

Maximum and minimum frequency values over the windows were {50.4, 49.58} Hz for input cases 1 and 2 and {50.2, 49.75} Hz for input case 3, respectively. Maximum and minimum RoCoF values (maximum FFD and minimum FFR) over the windows were {34.9, −28.4} mHz/s for input cases 1 and 2 and {54.33, −64} mHz/min, for input cases 1, 2, and 3, respectively, whose could be due to big sudden events. According to the set of (R100, R98, R90, R80), especially for R100 (highest value minus lowest value), the frequency deviates within the range of 0.05–0.25 Hz (for input case 1), 0.05–0.35 Hz (for input case 2) and 0–0.25 Hz (for input case 3). According to Tables 2 to 4, the over-deviation indices more often dominate the under-deviation indices because more windows have shown a higher over-deviation value than the under-deviation values. Opposite results were observed for the sub-10-min rms voltages in ref. [29]. VSV and Std. change within the ranges of 0.01–0.08 Hz and 0.01–0.06 Hz (input case 1), 0.01–0.1 Hz and 0.01–0.08 Hz (input case 2) and 0–0.09 Hz and 0–0.08 Hz (input case 3). The OF1 and UF1 are more common in terms of occurring within the windows for all input cases. NOF1 values are higher than NUF1 for the percentiles higher than the median, and in general, the over-frequency values slightly dominate the under-frequency values for input cases 1 and 2. For case 3, the situation is different, and NUF is higher than NOF (for all three thresholds), and it shows that the under-frequency happens more within the sub-1-hr windows with 3-min resolutions. The NFFD1 are very similar to NFFR1, and they vary within the range of 1–14 (for 80% of windows in input case 1), 1–40 (for whole windows in input case 2), and 1–7 (for whole windows in input case 3). 55% of the windows were detected as a low fluctuation (for all three input cases), 35% (for input cases 1 and 2) and 41% (for input case 3) as medium fluctuation, and 10% (for input case 1 and 2) and 4% (for input case 3) as high fluctuation. The quartile detected a greater number of outliers as 1–10 (for about 40% of windows in input case 1), 1–30 (for 70% of windows in input case 2), and 1–7 (for only about 22% of windows in input case 3).

b. *In terms of the extracted patterns*

For input cases 1 and 2, regardless of the window length, 6 patterns were extracted from k-means and k-medoids, while 7 patterns were extracted for input case 3 since the dataset belongs to a whole year compared to the other input cases. However, we can call it that about 6 or 7 "typical patterns" are extracted for the short time scales of frequency values. The sudden drops/rises in 10-s values are observed in almost all the patterns for input cases 1 and 2 but are less visible in sub-1-hr compared with sub-15-min windows. The sub-1-hr patterns for input case 3 somehow have a smoothed average of the patterns for input case 2 since the window length is similar, but the time resolution is bigger. In general, most of the extracted patterns for all the input cases were linked to the realities we discovered due to pre-knowledge labeling and some of them (downward patterns) are extracted specifically for the selected window length, i.e., sub-15-min and sub-1-hr windows.

5.6. Possible applications and benefits

According to the [61,62], all installed components in the transmission and distribution systems (including microgrids) should be able to operate within the defined requirements of frequency and time duration. Furthermore, to create a smarter grid, bridging the interface between policymakers and system operators is essential to achieving electricity balancing market goals [63,64]. However, the market-based operation can reduce frequency quality due to fixed production and/or control unit activation times (ramping 5–15 min before and after a clock hour), which should be further investigated using the proposed approach to develop mitigation techniques. Moreover, a fast frequency response of converter-interfaced control units can also affect frequency quality. Therefore, in addition to quantifying the frequency quality and extracting typical patterns within the sub-15-min and sub-1-hr intervals, this section discusses possible applications and benefits of the indices and patterns, as follows:

- Utilizing the discussed or proposed statistical indices in the power-quality monitors, particularly for frequency quality, as opposed to solely relying on aggregated values over time intervals, such as the duration required to restore the frequency, to capture crucial characteristics of the windows.

- Recommending the network operators to monitor the frequency trends using the statistical indices suggested and/or applied in this work, along with the "6 or 7 extracted typical patterns" extracted from sub-15-min and sub-1-hr intervals. They may use the "15 most

dominant ones" discussed in 5.1. The same approach was shown in our previous work [45] for some of the sub-10-min statistical indices R90, P95, P5, and Std. ([45], Fig. 17) as well as for the sub-10-min patterns extracted from a k-means clustering ([45], Fig. 19) for a 35-h recorded rms voltage.

- Using proposed frequency quality indices to adapt frequency control parameters in a control area, e.g., regulating reserves, frequency droop of control units, or secondary control frequency bias.
- Using typical frequency patterns to design mitigation techniques due to the disturbing impact of the flexible and fast operation of residential and industrial loads, distributed generations, and battery energy storage systems. A simple solution could be to limit the rate of change in the response of such units.
- Counseling power unit owners to adhere to dominant frequency quality indices and typical patterns as part of informational requirements during operational equipment stages.
- Counseling power unit designers to incorporate dominant frequency quality indices and typical patterns as part of preventive requirements and standards during equipment design stages.
- Using fast frequency rise and drop indices to detect critical RoCoF values and help prevent unintended grid splitting or enable intentional grid splitting. However, this application requires shorter time sampling and time windows.
- Utilizing the information obtained within the short time scales for data exchange between transmission system operators and distribution and microgrid operators. One solution can be a decision logic to prevent possible unintentional grid splitting or trigger intentional grid splitting to preserve stable operation.
- Application of the indices coupled with two recent real-world events: The first case occurred on March 28, 2023, as an under-frequency event [65], in which frequency was below 49.9 Hz between 16:55–17:01 (about six minutes) and a frequency drop to 49.87 Hz was observed at 16:59:58 in the Swedish power grid. Although the 49.87 Hz is not an extreme event, the proposed indices can detect it online or later in the postprocessing analysis. The second case occurred on June 8, 2023, at 12:39 a.m., when an over-frequency event occurred in the Nordic synchronous area [60,65]. The frequency abruptly increased to 50.5 Hz with a 10-second time resolution. Concurrently, an over-voltage event took place, resulting in the tripping of certain solar generators, as the network operators reported. Subsequently, the frequency rapidly dropped to 50.21 Hz and exhibited some fluctuations around that value until 12:46 p.m. At 12:47 p.m., the frequency returned to a safe range below 50.1 Hz and fluctuated around that level. After 12:50 p.m., the frequency remained within the safe range. During the recorded 15-minute window from 12:35–12:50 p.m., a frequency step was observed. At 12:39 p.m., the frequency abruptly rose from 50.1 Hz to 50.25 Hz, and at 12:46 p.m., it suddenly dropped from 50.2 Hz to 50.1 Hz. In addition to the indices proposed in this study, an index specifically designed to detect such frequency steps within short time windows could also provide further insight into the nature of these variations. However, it should be noted that time resolutions of less than 10 seconds are typically required to accurately capture such frequency steps [68].
- An important benefit of this study: Compared to looking at the frequency of high-resolution values, the processing is much easier, and there is no need to have storage with the capacity for huge amounts of data. This is mainly because of compressing the windows using the statistical indices and converting the windows into pattern-based windows, as discussed in 5.1.

Generally, the frequency quality is considered good enough by electricity customers. Large customers, such as mechanical paper industries and large generators, may be sensitive to the RoCoF. Discussed FFR and FFD can be used to detect critical RoCoF values; however, the time resolution and time window should be shorter than the ones discussed in this paper.

5.7. Recommendations for future work

The statistical indices suggested and proposed in this paper were derived by analyzing frequency records using insights from power-quality-based indices introduced in [29] and frequency-quality indices outlined in [1]. Furthermore, the extracted patterns benefited from the effective operation of clustering methods, which group data sets without prior knowledge while also leveraging the expertise of load-frequency experts regarding frequency variations (choosing the number of clusters). Based on our findings, we recommend the following areas for future work:

- One application of positive and negative peak detection with a predefined threshold has been reported in the medical field, such as infant breath detection [66]. In this paper, the index quantifying fluctuations was almost similarly extracted based on the total number of positive and negative peaks per window by fitting a threshold of 0.01%. However, different methods can be studied to quantify fluctuation levels.
- Three basic methods were used for quantifying the outliers, but there is potential to use other methods. One is to use machine learning methods to find the outliers per window and also to find the windows known as outliers in a set of datasets.
- According to [1], a possible frequency-quality index could be a combination of "maximum instantaneous frequency deviations" (MIFD) and "maximum steady-state frequency deviations" (MSFD) from the nominal frequency calculated for each of the windows (if there are the instantaneous and steady-state deviations) defined in this study. This can be shown as [|MSFD/MIFD| × 100] or [1 - |MSFD/MIFD|]. However, Std and VSV discussed in our study provided sufficient information regarding frequency deviations.
- The best time resolution used in this work, according to the used power-quality monitor, was 10 s. However, measurements with the highest resolution, e.g., 20 ms (PMU data), can be used to quantify the variations and patterns within the defined windows, extracting more information from the windows.
- To extract frequency patterns within short time windows, the well-known k-means/k-medoids clustering methods were used. The authors of this study aim to use a kernel principal component analysis (KPCA) or a deep autoencoder (DAE) to first reduce the size of frequency vectors with the dimensions (features) from high dimensions (90, 360, and 20 features in this study into principal features). The next step is to apply these reduced principal features to the k-means/k-medoids clustering methods. This approach may enable grouping different clusters, extraction of more information, and fluctuations in the extracted patterns, and, as a result, more real typical patterns may be identified.
- Apart from the unsupervised approach used in this work to extract short-scale time patterns, one can use higher resolution frequency samples over a longer period of time and also identify the reasons behind the frequency deviations per window. This approach could lead to labeling the windows and turning the problem into a supervised one, thereby identifying more real patterns per window.
- Given the reasons in 5.3, the 15 min and 1 hr windows were chosen in this study. However, the authors recommend conducting experiments with different window lengths between 5 min, 10 min, 15 min, 30 min, and 1 hr. This could be done by considering frequency control requirements and the time durations to recover frequency values after small and large disturbances/events.
- The statistical indices used in this work may be used as additional features to increase the length of the windows n in the input cases. As part of a feature engineering approach, the improved windows may help the clustering methods to group the windows more accurately and, consequently, identify more real excluded patterns.
- A supervised deep learning method similar to the one reviewed in (5.1, [49]), can utilize the indices quantifying events (as discussed in

2.1.2) to detect events that occur within the short time scales. This requires collecting data that include the indices and the corresponding labeled events.
- The correlations used in 5.4 were calculated using the Pearson method. However, cross-correlation analysis can also be used, considering the time shift (lag) between patterns to evaluate the effectiveness of the clustering methods.
- After quantifying the frequency-quality indices and extracting typical patterns, the next step could be to study the possible impact of poor frequency quality on power generation units in time scales below 15 min and 1 hr.
- The proposed indices and the method to extract the typical patterns are not reliant on specific measurement data from a particular power system, presenting the broad applicability of the approaches. However, when applying the proposed indices and unsupervised pattern extraction methods in a different power system (synchronous area), it is important to consider the potential need for updating the thresholds specified in Table 2.
- Investigating the impact of climate change on electrical power and energy systems involves examining variables such as electricity demand and frequency patterns [67]. Therefore, a potential future research direction could involve analyzing these impacts on the extraction of frequency patterns within short time scales.

6. Conclusion

This paper addresses the absence of short-time scales' analysis for frequency values in grid codes. Its objectives are quantifying frequency quality in terms of variations, events, fluctuations, and outliers and extracting frequency trend patterns within short time scales, below one hour, such as sub-15-min and sub-1-hr time scales. Next to the 23 selected statistical indices, another 13 indices were proposed for use on short-time scales. Additional 12 indices (out of which 5 are proposed) were identified as the most dominant. Results obtained for three different input cases are summarized as follows:

- The maximum frequency values' deviation over the windows was 0.35 Hz for cases 1 and 2 and 0.25 Hz for case 3 (based on the R100 index).
- Over-deviation indices more often dominated under-deviation indices, and over- and under-frequencies with a threshold of 0.1% were more common within the mentioned windows.
- Over-frequency values dominated slightly under-frequency values for cases 1 and 2, while the opposite was observed for case 3.
- The number of fast-frequency drops/rises had similar cumulative distribution functions with different ranges for the input cases.
- In terms of fluctuation level over the windows, 10% of the windows (for cases 1 and 2) and 4% (for case 3) were detected as high fluctuation.
- The quartile method detected a greater number of outliers for a maximum of about 40% of windows in input case 1, 70% of windows in input case 2, and only about 22% of windows in input case 3.

While the statistical results vary notably between cases 1 and 2 compared to case 3, they all demonstrate the occurrence of significant variations within the short time windows. Furthermore, around 6 or 7 typical patterns were extracted within short time windows when applying the presented unsupervised scheme. It should be noted that when the short time scales have higher time resolutions, typically within a few seconds, the extracted patterns reveal the ability to detect and show sudden drops successfully or rises in frequency instants (cases 1 and 2). Therefore, the authors advocate for greater attention to these time scales within which significant events can occur. The proposed approaches can aid in achieving market goals and improving balancing processes between generation and consumption. Efficient monitoring of frequency trends using dominant indices and patterns is recommended for network operators, while power unit owners/designers should incorporate these measures into operational and design stages. Moreover, information exchange among system operators regarding frequency indices and patterns can also enhance grid resilience. The approaches used to obtain the results in this study remain consistent across cases 1–3. However, it is important to note that a network operator typically focuses on a specific case of interest rather than analyzing all cases collectively.

Generally, the approach presented in this work can be useful for standardization efforts in the quantification of power system frequency in terms of "quality" and "trend" in short time scales. The authors realize that this study is a preliminary step in understanding frequency behaviors in specific time scales and can lead to further analysis.

Authorship statement

All authors certify that they have participated sufficiently in work to take public responsibility for the content, including participation in the manuscript's concept, design, analysis, writing, or revision. Furthermore, each author certifies that this material or similar material has not been and will not be submitted to or published in any other publication before its appearance in the SEGAN.

CRediT authorship contribution statement

Davood Khodadad: Funding acquisition, Supervision, Writing – review & editing. **Roberto Chouhy Leborgne:** Writing – review & editing. **Boštjan Polajžer:** Conceptualization, Investigation, Writing – review & editing. **Younes Mohammadi:** Conceptualization, Data curation, Investigation, Methodology, Software, Validation, Writing – original draft, Writing – review & editing.

Declaration of Competing Interest

The authors declare that they have no known competing financial interests or personal relationships that could have appeared to influence the work reported in this paper.

Data Availability

Data will be made available on request.

Acknowledgment

The authors would like to thank the funding support from the Kempe Foundation (Kempestiftelserna) for grant number JCK22–0025, Sweden. This work has been also supported by the ARIS under project number P2-0115, Slovenia. The authors would like to express their gratitude to Prof. Math H. J. Bollen, the head of the Electrical Power Engineering subject at Luleå University of Technology, Sweden, for his previous valuable guidance regarding frequency quality indices and for granting permission to utilize the recorded data collected by the power quality monitor (Metrum PQsmart).

References

[1] EUR-Lex - 32017R1485 - EN - EUR-Lex n.d. ⟨https://eur-lex.europa.eu/legal-content/EN/TXT/?uri=CELEX%3A32017R1485⟩ (Accessed March 3, 2023).
[2] NERC, Fast frequency response concepts and bulk power system reliability needs, NERC Invert. -Based Resour. Perform. Task. Force (2020) 1–23.
[3] N.W. Miller, M. Shao, R. D'aquila, S. Pajic, K. Clark, Frequency response of the US Eastern interconnection under conditions of high wind and solar generation, Seven. Annu. IEEE Green. Technol. Conf. 2015 (2015) 21–28, https://doi.org/10.1109/GREENTECH.2015.31.
[4] A. Egorov, A. Savosina, M. Sadokhina, Research of the number and installed capacity of solar and wind power plants in interregional and regional power systems in the Russian UPS, 2021 Ural. Smart Energy Conf. (2021) 152–156, https://doi.org/10.1109/USSEC53120.2021.9655764.

[5] Adu J.A., Napolitano F., Penaloza J.D.R., Pontecorvo T., Tossani F. Influence of Fast Frequency Response Services in DFIG-Based Wind Power Plants on Power Grids Stability. 2020 IEEE Int. Conf. Environ. Electr. Eng. 2020 IEEE Ind. Commer. Power Syst. Eur. (EEEIC / I&CPS Eur., 2020, p. 1–6. https://doi.org/10.1109/EEEIC/ICPSEurope49358.2020.9160628.

[6] (IEC) IEC. Electromagnetic compatibility (EMC)-Part 4–30: Testing and measurement techniques-Power quality measurement methods. IEC 61000–4-30 2003.

[7] Z. Xu, J. Ostergaard, M. Togeby, F.R. Isleifsson, Evaluating frequency quality of nordic system using PMU data, IEEE Power Energy Soc. Gen. Meet. Convers. Deliv. Electr. Energy 21st Century 2008 (2008) 1–5, https://doi.org/10.1109/PES.2008.4596468.

[8] Fingrid, Freq. Qual. Anal. 2021 (2021).

[9] M. Persson, P. Chen, Frequency evaluation of the Nordic power system using PMU measurements, IET Gener. Transm. Distrib. 11 (2017) 2879–2887, https://doi.org/10.1049/iet-gtd.2017.0095.

[10] D. Zografos, M. Ghandhari, 2019, Power System Inertia Estimation and Frequency Response Assessment.

[11] H. Zbigniew, A. Bien, Voltage disturbances, Power Qual. Appl. Guid (2006).

[12] NordelNordel. Nordic Grid Code 2007 2007;2007:69–74.

[13] Nordic System Operation Workshop ENTSO-E: a pan-European TSO platform, fully operational since 1 July 2009. System 2010..

[14] European Network of Transmission System Operators for Electricity From: Incident Classification Scale Subgroup 2022..

[15] NERC n.d. ⟨https://www.nerc.com/Pages/default.aspx⟩ (Accessed February 11, 2023).

[16] C.-I. Chen, Y.-C. Chen, Comparative study of harmonic and interharmonic estimation methods for stationary and time-varying signals, IEEE Trans. Ind. Electron 61 (2014) 397–404, https://doi.org/10.1109/TIE.2013.2242419.

[17] S.L. Braide, Evaluation and analysis of harmonic distortion on 330kV network case study selected sub-region Nigerian power system for improve power quality, J. Prog. Eng. Phys. Sci. 1 (2022) 13–22, https://doi.org/10.56397/jpeps.2022.11.03.

[18] D. Belega, D. Petri, Accurate frequency estimation of electrical waveforms affected by harmonics and interharmonics, 2022 IEEE 21st Mediterr. Electrotech. Conf. (2022) 1097–1101, https://doi.org/10.1109/MELECON53508.2022.9842877.

[19] A. Eslami, M. Negnevitsky, E. Franklin, S. Lyden, An intelligent active power filter to mitigate harmonics and interharmonics, 2022 20th Int. Conf. Harmon. Qual. Power (2022) 1–6, https://doi.org/10.1109/ICHQP53011.2022.9808722.

[20] M.H. Moradi, Y. Mohammadi, M. Hoseyni Tayyebi, A novel method to locate the voltage sag source: A case study in the Brazilian power network (Mato Grosso), Prz. Elektrotech. 88 (2012) 112–115.

[21] Y. Mohammadi, R.C. Leborgne, Relative location of voltage sags source at the point of common coupling of constant power loads in distribution systems, Int Trans. Electr. Energy Syst. 30 (2020) 1–15, https://doi.org/10.1002/2050-7038.12516.

[22] Y. Mohammadi, R.C. Leborgne, B. Polajžer, Modified methods for voltage-sag source detection using transient periods, Electr. Power Syst. Res. 207 (2022) 107857, https://doi.org/10.1016/j.epsr.2022.107857.

[23] Y. Mohammadi, A. Salarpour, R. Chouhy Leborgne, Comprehensive strategy for classification of voltage sags source location using optimal feature selection applied to support vector machine and ensemble techniques, Int J. Electr. Power Energy Syst. 124 (2021) 106363, https://doi.org/10.1016/j.ijepes.2020.106363.

[24] P. Caramia, G. Carpinelli, P. Verde, Power quality indices in liberalized markets, Wiley, 2009.

[25] L. Soder, M. Amelin, Effic. Oper. Plan. Power Syst. (2011) 230.

[26] S. Färegård, M. Miletic, A Swedish perspective on aggregators and local flexibility markets considerations and barriers for aggregators and SthlmFlex together with their potential to manage grid congestions in Stockholm, Degree Proj. Energy Environ. (2021).

[27] NTSO-E. Nordic Balancing Philosophy 2016-06-2016 2016.

[28] U. Farooq, R.B. Bass, Frequency event detection and mitigation in power systems: a systematic literature review, IEEE Access 10 (2022) 61494–61519, https://doi.org/10.1109/ACCESS.2022.3180349.

[29] M. Bollen, A.G. de Castro, S. Rönnberg, Characterization methods and typical levels of variations in rms voltage at the time scale between 1 second and 10 min, Electr. Power Syst. Res. 184 (2020) 106322, https://doi.org/10.1016/j.epsr.2020.106322.

[30] A. Gil-de-Castro, M.H.J. Bollen, S.K. Rönnberg, Variations in harmonic voltage at the sub-10-minute time scale, Electr. Power Syst. Res 195 (2021) 107163, https://doi.org/10.1016/j.epsr.2021.107163.

[31] X. Dominguez, A. Prado, P. Arboleya, V. Terzija, Evolution of knowledge mining from data in power systems: the big data analytics breakthrough, Electr. Power Syst. Res. 218 (2023) 109193, https://doi.org/10.1016/J.EPSR.2023.109193.

[32] G. Chaoyu, Z. Su, P. Wang, Y. You, Distributed evidential clustering toward time series with big data issue, Expert Syst. Appl. (2021), https://doi.org/10.1016/j.eswa.2021.116279.

[33] N. Alemazkoor, M. Tootkaboni, R. Nateghi, A. Louhghalam, Smart-meter big data for load forecasting: an alternative approach to clustering, IEEE Access 10 (2022) 8377–8387, https://doi.org/10.1109/ACCESS.2022.3142680.

[34] S.E. Haupt, B. Kosović, Variable generation power forecasting as a big data problem, IEEE Trans. Sustain Energy 8 (2017) 725–732, https://doi.org/10.1109/TSTE.2016.2604679.

[35] L. Wen, K. Zhou, S. Yang, A shape-based clustering method for pattern recognition of residential electricity consumption, J. Clean. Prod. 212 (2019) 475–488, https://doi.org/10.1016/j.jclepro.2018.12.067.

[36] H. Izakian, W. Pedrycz, I. Jamal, Fuzzy clustering of time series data using dynamic time warping distance, Eng. Appl. Artif. Intell. 39 (2015) 235–244, https://doi.org/10.1016/j.engappai.2014.12.015.

[37] P. Arora, S. Varshney, Analysis of k-means and k-medoids algorithm for big data, Procedia Comput. Sci. 78 (2016) 507–512.

[38] N. Sureja, B. Chawda, A. Vasant, An improved K-medoids clustering approach based on the crow search algorithm, J. Comput. Math. Data Sci. 3 (2022) 100034, https://doi.org/10.1016/j.jcmds.2022.100034.

[39] L.G.B. Ruiz, M.C. Pegalajar, R. Arcucci, M. Molina-Solana, A time-series clustering methodology for knowledge extraction in energy consumption data, Expert Syst. Appl. 160 (2020) 113731, https://doi.org/10.1016/j.eswa.2020.113731.

[40] A.E. Lazzaretti, V.H. Ferreira, H.V. Neto, New trends in power quality event analysis: novelty detection and unsupervised classification, J. Control Autom. Electr. Syst. 27 (2016) 718–727, https://doi.org/10.1007/s40313-016-0265-z.

[41] M. Dey, S.P. Rana, C.V. Simmons, S. Dudley, Solar farm voltage anomaly detection using high-resolution μPMU data-driven unsupervised machine learning, Appl. Energy 303 (2021) 117656, https://doi.org/10.1016/j.apenergy.2021.117656.

[42] A. Eslami, M. Negnevitsky, E. Franklin, S. Lyden, Review of AI applications in harmonic analysis in power systems, Renew. Sustain Energy Rev. 154 (2022) 111897, https://doi.org/10.1016/j.rser.2021.111897.

[43] Aligholian A. Unsupervised Data-Driven Event Analysis of Smart Grid Time-Series 2022. https://doi.org/https://escholarship.org/uc/item/94n5r7b4..

[44] Y. Mohammadi, S.M. Miraftabzadeh, M.H.J. Bollen, M. Longo, An unsupervised learning schema for seeking patterns in rms voltage variations at the sub-10-minute time scale, Sustain Energy, Grids Netw. 31 (2022) 100773, https://doi.org/10.1016/j.segan.2022.100773.

[45] Y. Mohammadi, S. Mahdi Miraftabzadeh, M.H.J. Bollen, M. Longo, Seeking patterns in rms voltage variations at the sub-10-minute scale from multiple locations via unsupervised learning and patterns' post-processing, Int J. Electr. Power Energy Syst. 143 (2022), https://doi.org/10.1016/j.ijepes.2022.108516.

[46] D.O. Koval, Power system disturbance patterns, IEEE Trans. Ind. Appl. 26 (1990) 556–562, https://doi.org/10.1109/28.55958.

[47] S.V. Verdu, M.O. Garcia, C. Senabre, A.G. Marin, F.J.G. Franco, Classification, filtering, and identification of electrical customer load patterns through the use of self-organizing maps, IEEE Trans. Power Syst. 21 (2006) 1672–1682, https://doi.org/10.1109/TPWRS.2006.881133.

[48] E. Carpaneto, G. Chicco, R. Napoli, M. Scutariu, Electricity customer classification using frequency–domain load pattern data, Int J. Electr. Power Energy Syst. 28 (2006) 13–20, https://doi.org/10.1016/j.ijepes.2005.08.017.

[49] Y. Zhang, X. Shi, H. Zhang, Y. Cao, V. Terzija, Review on deep learning applications in frequency analysis and control of modern power system, Int J. Electr. Power Energy Syst. 136 (2022) 107744, https://doi.org/10.1016/j.ijepes.2021.107744.

[50] Y. Mohammadi, S.M. Miraftabzadeh, M.H.J. Bollen, M. Longo, Voltage-sag source detection: developing supervised methods and proposing a new unsupervised learning, Sustain Energy, Grids Netw. 32 (2022) 100855, https://doi.org/10.1016/J.SEGAN.2022.100855.

[51] M.H.J. Bollen, M. Häger, C. Schwaegerl, Quantifying voltage variations on a time scale between 3 seconds and 10 min, IEE Conf. Publ. 2 (2005) 413–417, https://doi.org/10.1049/cp:20051076.

[52] NIST/SEMATECH e-Handbook of Statistical Methods. n.d. https://doi.org/https://doi.org/10.18434/M32189.

[53] A. Bagnall, J. Lines, A. Bostrom, J. Large, E. Keogh, The great time series classification bake off: a review and experimental evaluation of recent algorithmic advances, Data Min. Knowl. Discov. 31 (2017) 606–660, https://doi.org/10.1007/s10618-016-0483-9.

[54] A.K. Jain, R.C. Dubes, Algorithms for clustering data, Prentice-Hall, Inc, 1988.

[55] K.P. Sinaga, M.S. Yang, Unsupervised K-means clustering algorithm, IEEE Access 8 (2020) 80716–80727, https://doi.org/10.1109/ACCESS.2020.2988796.

[56] L. Kaufman, P.J. Rousseeuw, Partitioning around medoids (program pam), Find. Groups Data Introd. Clust. Anal. 344 (1990) 68–125.

[57] D. Arthur, S. Vassilvitskii, K-means++: the advantages of careful seeding, Proc. Annu ACM-SIAM Symp. Discret Algorithms (2007) 1027–1035, 07-09-Janu.

[58] L. Van Der Maaten, G. Hinton, Visualizing data using t-SNE, J. Mach. Learn Res. 9 (2008) 2579–2625.

[59] Homepage of Fingrid - Open data - Download datasets n.d. ⟨https://data.fingrid.fi/en/data?datasets=177⟩ (Accessed February 11, 2023).

[60] Fingrid api search n.d. ⟨https://data.fingrid.fi/open-data-forms/search/en/?selected_datasets=177⟩ (Accessed February 11, 2023).

[61] Frequency ranges ENTSO-E guidance document for national implementation of frequency ranges for network codes on grid connection Prepared from: StG CNC n.d..

[62] P.R. Version, M. Håberg, K.H. StatnettFrequency Quality, phase 2, 2017, p. 1–44.

[63] ENTSO-E, Towards smarter grids: developing TSO and DSO roles and interactions for the benefit of consumers. Eur. Netw. Transm. Syst. Oper. Electr. (2015) 1–8.

[64] M. Radi, G. Taylor, J. Cantenot, E. Lambert, N. Suljanovic, Developing enhanced TSO-DSO information and data exchange based on a novel use case methodology, Front Energy Res. 9 (2021) 1–15, https://doi.org/10.3389/fenrg.2021.670573.

[65] The control room | Svenska kraftnät n.d. ⟨https://www.svk.se/en/national-grid/the-control-room/⟩ (Accessed April 11, 2023).

[66] D. Khodadad, S. Nordebo, B. Müller, A. Waldmann, R. Yerworth, T. Becher, et al., Optimized breath detection algorithm in electrical impedance tomography, Physiol. Meas. 39 (2018) 94001, https://doi.org/10.1088/1361-6579/aad7e6.

[67] Y. Mohammadi, A. Palstev, B. Polajžer, S.M. Miraftabzadeh, D. Khodadad, Investigating winter temperatures in Sweden and Norway: potential relationships with climatic indices and effects on electrical power and energy systems, Energies 16 (2023), https://doi.org/10.3390/en16145575.

[68] Frequency - historical data (fingrid.fi).